GRX-overexpressing cells, the enhancing effect of PTPI-III on the PDGF-induced phosphorylation of PDGFRβ was consistent with the data using siRNA for LMW-PTP. However, at present it is not clear why suppression of endogenous LMW-PTP by PTPI-III does not much influence on the PDGF-BB-induced phosphorylation of PDGFRβ in control cells. It is reported that α-bromoacetophenone derivatives such as PTPI-III act as PTP inhibitors by covalently alkylating the conserved catalytic Cys residue in the PTP active site (58). In this respect it is possible that the susceptibility of endogenous LMW-PTP to PTPI-III could be changed when the redox state of endogenous LMW-PTP is different between control and GRX-overexpressing cells. This suggests that the effect of PTPI-III on endogenous LMW-PTP may be highly enhanced in GRX-overexpressing cells compared with controls.

LMW-PTP is an 18-kDa enzyme that is widely expressed (39, 59). Previous studies on the molecular biology of LMW-PTP in NIH3T3 cells demonstrated a well defined role for this enzyme in PDGF-BB-induced mitogenesis showing that activated PDGFRβ is a substrate for LMW-PTP (56). We showed that cellular LMW-PTP was inactivated by peroxide, which could be generated with PDGF-BB, and the inactivation was suppressed by antioxidants such as Trolox or NAC (Figs. 5, *B* and *C*). These results support previous findings that LMW-PTP is oxidized by ROS generated in cells stimulated with PDGF-BB, resulting in up-regulation of the phosphorylation of PDGFRβ. We also showed that GRX could up-regulate the activity of LMW-PTP even in the cells treated with PDGF-BB, resulting in an enhanced dephosphorylation of PDGFRβ. Furthermore, *in vitro* we found that treatment with H_2O_2 causes the formation of high molecular weight oligomers of LMW-PTP in SDS-PAGE under non-reducing conditions. The high molecular weight form disappeared and shifted to a single molecule of 25 kDa in SDS-PAGE under reducing conditions. This suggested that LMW-PTP forms DTT-reducible oligomers *in vitro* through oxidation-induced disulfide-bond formation between the molecules. In the presence of GRX- and GSH-regenerating systems, the H_2O_2-induced oligomer formation of LMW-PTP was apparently suppressed, and the activity of LMW-PTP was also protected from H_2O_2-induced inactivation. Collectively, these results indicate that GSH/GRX systems effectively work to protect against oxidation-dependent structural change and inactivation of LMW-PTP.

During PDGF signaling, LMW-PTP is regulated by a redox-dependent mechanism involving the two Cys residues of the catalytic site, which change reversibly from the reduced to oxidized state after PDGF treatment. The reversibility of *in vivo* LMW-PTP oxidation is glutathione-dependent (35). The additional catalytic Cys-17 retains an interesting role in the formation of the S-S intramolecular bond, which protects the catalytic Cys-12 from further and irreversible oxidation. The presence of an additional Cys near the catalytic one confers upon LMW-PTP the ability to rapidly recover its activity and finely regulate PDGF receptor activation. To investigate whether specific Cys residues of the catalytic site of LMW-PTP are involved in the oxidation-induced oligomer formation of LMW-PTP *in vitro*, the LMW-PTP mutant, in which Cys-17 was changed to Ser by site-directed mutagenesis, was produced and characterized by non-reducing SDS-PAGE after treatment with H_2O_2. The results showed that high molecular weight oligomers were formed by H_2O_2 even with the mutant LMW-PTP, indicating that Cys-17 had no particular contribution to oxidation-induced oligomer formation (data not shown). This suggests that there is no direct correlation between the inactivation status and formation of high molecular weight oligomers of LMW-PTP under conditions with H_2O_2 *in vitro*, although oxidation-induced oligomer formation was effectively suppressed by GRX- and GSH-regeneration systems. It is also noteworthy that the oxidation-induced oligomer formation of LMW-PTP was not detected in non-reducing SDS-PAGE of cell lysate samples from LMW-PTP gene-transfected cells treated with H_2O_2 (data not shown). Thus, further investigation is required to clarify precise mechanical correlation between the activation status and structure of LMW-PTP in cells treated with PDGF.

PTP-1B has been extensively studied in terms of its redox-dependent regulation related to the signaling receptors for epidermal growth factor (44, 60) and insulin (61, 62). The oxidation state of the active-Cys in PTP1B was also clearly characterized by structural analyses (63, 64). PTP1B has been reported to be involved in the redox-dependent dephosphorylation of PDGFR. Lee *et al.* (19) reported that oxidized PTP-1B is reduced by TRX rather than GSH/GRX systems. On the other hand, Barrett *et al.* (65) reported that GSH could recycle oxidized PTP1B, showing the involvement of GSH-related systems in the mechanism. Thus, the precise mechanism of the redox regulation of PTP-1B is still controversial: SHP-2 is also an example of a redox-regulated PTP involved in the PDGFR signaling (52). Recently, the tumor suppressor protein, PTEN (phosphate and tensin homolog deleted on chromosome ten), has also been reported to dephosphorylate PDGFR (66). Although the activity of PTEN is regulated in a redox-dependent manner, oxidized PTEN is reduced by TRX rather than GRX *in vitro* (67). In the present study the expression of TRX was slightly suppressed in the GRX-overexpressing cells compared with controls (data not shown), but its relation to the redox-dependent regulation of LMW-PTP was not elucidated. On the other hand, in the case of mouse embryonic fibroblasts in which the PTP-1B gene was knocked out, the phosphorylation status of PDGFRβ was not much influenced by stimulation with PDGF-BB, suggesting that other PTPs could compensate for the loss of PTP-1B function (68). Taken together, these findings suggest that several different PTPs are involved in the redox-dependent regulation of the dephosphorylation of phosphorylated PDGFR. Thus, to clarify the precise mechanism behind the regulation of PDGF signaling, further investigations are required. In conclusion, the present study shows that GRX and GSH-regenerating systems are involved in the regulation of PDGF-BB signaling through the redox-dependent regulation of LMW-PTP.

Acknowledgment—We are grateful to Midori Ikezaki and Akiko Emura for technical assistance.

REFERENCES

1. Holmgren, A. (1989) *J. Biol. Chem.* **264**, 13963–13966
2. Holmgren, A. (1976) *Proc. Natl. Acad. Sci. U. S. A.* **73**, 2275–2279

3. Gravina, S. A., and Mieyal, J. J. (1993) *Biochemistry* **32,** 3368–3376
4. Shelton, M. D., Chock, P. B., and Mieyal, J. J. (2005) *Antioxid. Redox Signal.* **7,** 348–366
5. Holmgren, A. (1979) *J. Biol. Chem.* **254,** 3672–3678
6. Gan, Z.-R., and Wells, W. W. (1986) *J. Biol. Chem.* **261,** 996–1001
7. Prinz, W. A., Aslund, F., Holmgren, A., and Beckwith, J. (1997) *J. Biol. Chem.* **272,** 15661–15667
8. Casagrande, S., Bonetto, V., Fratelli, M., Gianazza, E., Eberini, I., Massignan, T., Salmona, M., Chang, G., Holmgren, A., and Ghezzi, P. (2002) *Proc. Natl. Acad. Sci. U. S. A.* **99,** 9745–9749
9. Davis, D. A., Newcomb, F. M., Starke, D. W., Ott, D. E., Mieyal, J. J., and Yarchoan, R. (1997) *J. Biol. Chem.* **272,** 25935–25940
10. Lind, C., Gerdes, R., Schuppe-Koistinen, I., and Cotgreave, I. A. (1998) *Biochem. Biophys. Res. Commun.* **247,** 481–486
11. Bandyopadhyay, S., Starke, D. W., Mieyal, J. J., and Gronostajski, R. M. (1998) *J. Biol. Chem.* **273,** 392–397
12. Song, J. J., Rhee, J. G., Suntharalingam, M., Walsh, S. A., Spitz, D. R., and Lee, Y. J. (2002) *J. Biol. Chem.* **277,** 46566–46575
13. Kikawa, K. D., Vidale, D. R., Van Etten, R. L., and Kinch, M. S. (2002) *J. Biol. Chem.* **277,** 39274–39279
14. Wang, J., Tekle, E., Oubrahim, H., Mieyal, J. J., Stadtman, E. R., and Chock, P. B. (2003) *Proc. Natl. Acad. Sci. U. S. A.* **100,** 5103–5106
15. Adachi, T., Pimentel, D. R., Heibeck, T., Hou, X., Lee, Y. J., Jiang, B., Ido, Y., and Cohen, R. A. (2004) *J. Biol. Chem.* **279,** 29857–29862
16. Landino, L. M., Moynihan, K. L., Todd, J. V., and Kennett, K. L. (2004) *Biochem. Biophy. Res. Commun.* **314,** 555–560
17. Landino, L. M., Robinson, S. H., Skreslet, T. E., and Cabral, D. M. (2004) *Biochem. Biophy. Res. Commun.* **323,** 112–117
18. Caplan, J. F., Filipenko, N. R., Fitzpatrick, S. L., and Waisman, D. M. (2004) *J. Biol. Chem.* **279,** 7740–7750
19. Lee, S.-R., Kwon, K.-S., Kim, S.-R., and Rhee, S. G. (1998) *J. Biol. Chem.* **273,** 15366–15372
20. Murata, H., Ihara, Y., Nakamura, H., Yodoi, J., Sumikawa, K., and Kondo, T. (2003) *J. Biol. Chem.* **278,** 50226–50233
21. Johansson, C., Lillig, C. H., and Holmgren, A. (2004) *J. Biol. Chem.* **279,** 7537–7543
22. Beer, S. M., Taylor, E. R., Brown, S. E., Dahm, C. C., Costa, N. J., Runswick, M. J., and Murphy, M. P. (2004) *J. Biol. Chem.* **279,** 47939–47951
23. Lillig, C. H., Lonn, M. E., Enoksson, M., Fernandes, A. P., and Holmgren, A. (2004) *Proc. Natl. Acad. Sci. U. S. A.* **101,** 13227–13232
24. Tallquist, M., and Kazlauskas, A. (2004) *Cytokine Growth Factor Rev.* **15,** 205–213
25. Heldin, C.-H., and Westermark, B. (1999) *Physiol. Rev.* **79,** 1283–1316
26. Betsholtz, C. (2004) *Cytokine Growth Factor Rev.* **15,** 215–228
27. Leveen, P., Pekny, M., Gebre-Medhin, S., Swolin, B., Larsson, E., and Betsholtz, C. (1994) *Genes Dev.* **8,** 1857–1887
28. Soriano, P. (1994) *Genes Dev.* **8,** 1888–1896
29. Sarzani, R., Arnaldi, G., and Chobanian, A. V. (1991) *Hypertension* **17,** 888–895
30. Brostrom, M. A., Meiners, S., and Brostrom, C. O. (2002) *J. Cell. Biochem.* **84,** 736–749
31. Liu, J., Wu, L.-L., Li, L., Zhang, L., Song, Z-E. (2005) *Regul. Pept.* **127,** 11–18
32. Kageyama, K., Ihara, Y., Goto, S., Urata, Y., Toda, G., Yano, K., and Kondo, T. (2002) *J. Biol. Chem.* **277,** 19255–19264
33. Cirri, P., Caselli, A., Manao, G., Camici, G., Polidori, R., Cappugi, G., and Ramponi, G. (1995) *Biochim. Biophys. Acta* **1243,** 129–135
34. Wo, Y. Y., McCormack, A. L., Shabanowitz, J., Hunt, D. F., Davis, J. P., Mitchell, G. L., and Van Etten, R. L. (1992) *J. Biol. Chem.* **267,** 10856–10865
35. Chiarugi, P., Fiaschi, T., Taddei, M. L., Talini, D., Giannoni, E., Raugei, G., and Ramponi, G. (2001) *J. Biol. Chem.* **276,** 33478–33487
36. Chen, A., and Zhang, L. (2003) *J. Biol. Chem.* **278,** 23381–23389
37. Chiarugi, P., and Cirri, P. (2003) *Trends Biochem. Sci.* **28,** 509–514
38. Persson, C., Savenhed, C., Bourdeau, A., Tremblay, M. L., Markova, B., Bohmer, F.-D., Haj, F. G., Neel, B. G., Elson, A., Heldin, C.-H., Ronnstrand, L., Ostman, A., and Hellberg, C. (2004) *Mol. Cell. Biol.* **24,** 2190–2201
39. Raugei, G., Ramponi, G., and Chiarugi, P. (2002) *Cell. Mol. Life Sci.* **59,** 941–949
40. Arabaci, G., Guo, X.-C., Beebe, K. D., Coggeshall, K. M., and Pei, D. (1999) *J. Am. Chem. Soc.* **121,** 5085–5086
41. Chrestensen, C. A., Starke, D. W., and Mieyal, J. J. (2000) *J. Biol. Chem.* **275,** 26556–26565
42. Sundaresan, M., Yu, Z. X., Ferrans, V. J., Irani, K., and Finkel, T. (1995) *Science* **270,** 296–299
43. Brar, S. S., Kennedy, T. P., Whorton, A. R., Murphy, T. M., Chitano, P., and Hoidal, J. R. (1999) *J. Biol. Chem.* **274,** 20017–20026
44. Bae, Y. S., Kang, S. W., Seo, M. S., Baines, I. C., Tekle, E., Chock, P. B., and Rhee, S. G. (1997) *J. Biol. Chem.* **272,** 217–221
45. Tonks, N. K. (2005) *Cell* **121,** 667–670
46. Caselli, A., Chiarugi, P., Camici, G., Manao, G., and Ramponi, G. (1995) *FEBS Lett.* **374,** 249–252
47. Caselli, A., Marzocchini, R., Camici, G., Manao, G., Moneti, G., Pieraccini, G., and Ramponi, G. (1998) *J. Biol. Chem.* **273,** 32554–32560
48. Ostman, A., and Bohmer, F.-D. (2001) *Trends Cell Biol.* **11,** 258–266
49. Lambeth, J. D. (2004) *Nat. Rev. Immunol.* **4,** 181–189
50. Yu, Z., Su, L., Hoglinger, O., Jaramillo, M. L., Banville, D., and Shen, S.-H. (1998) *J. Biol. Chem.* **273,** 3687–3694
51. Kazlauskas, A., Feng, G.-S., Pawson, T., and Valius, M. (1993) *Proc. Natl. Acad. Sci. U. S. A.* **90,** 6939–6942
52. Meng, T.-C., Fukada, T., and Tonks, N. K. (2002) *Mol. Cell* **9,** 387–399
53. Haj, F. G., Verveer, P. J., Squire, A., Neel, B. G., and Bastiaens, P. I. H. (2002) *Science* **295,** 1708–1711
54. Markova, B., Herrlich, P., Ronnstrand, L., and Bohmer, F. D. (2003) *Biochemistry* **42,** 2691–2699
55. Kovalenko, M., Denner, K., Sandstrom, J., Persson, C., Grob, S., Jandt, E., Viella, R., Bohmer, F., and Ostman, A. (2000) *J. Biol. Chem.* **275,** 16219–16226
56. Chiarugi, P., Cirri, P., Raugei, G., Camici, G., Dolfi, F., Berti, A., and Ramponi, G. (1995) *FEBS Lett.* **372,** 49–53
57. Shimizu, H., Shiota, M., Yamada, N., Miyazaki, K., Ishida, N., Kim, S., and Miyazaki, H. (2001) *Biochem. Biophys. Res. Commun.* **289,** 602–607
58. Arabaci, G., Yi, T., Fu, H., Porter, M. E., Beebe, K. D., and Pei, D. (2002) *Bioorg. Med. Chem. Lett.* **12,** 3047–3050
59. Ramponi, G., and Stefani, M. (1997) *Biochim. Biophys. Acta* **1341,** 137–156
60. Liu, F., and Chernoff, J. (1997) *Biochem. J.* **327,** 139–145
61. Elchebly, M., Paytte, P., Michaliszyn, E., Cromlish, W., Collins, S., Loy, A. L., Normandin, D., Cheng, A., Himms-Hagen, J., Chan, C. C., Ramachandran, C., Gresser, M. J., Tremblay, M. L., and Kennedy, B. P. (1999) *Science* **283,** 1544–1548
62. Mahadev, K., Zilbering, A., Zhu, L., and Goldstein, B. J. (2001) *J. Biol. Chem.* **276,** 21938–21942
63. Van Montfort, R. L. M., Congreve, M., Tisi, D., Carr, R., and Jhoti, H. (2003) *Nature* **423,** 773–777
64. Salmeen, A., Anderson, J. N., Myers, M. P., Meng, T.-C., Hinks, J. A., Tonks, N. K., and Barford, D. (2003) *Nature* **423,** 769–773
65. Barrett, W. C., DeGnore, J. P., König, S., Fales, H. M., Keng, Y.-F., Zhang, Z.-Y., Yim, M. B., and Chock, P. B. (1999) *Biochemistry* **18,** 6699–6705
66. Mahimainathan, L., and Choudhury, G. G. (2004) *J. Biol. Chem.* **279,** 15258–15268
67. Lee, S.-R., Yang, H.-S., Kwon, J., Lee, C., Jeong, W., and Rhee, S. G. (2002) *J. Biol. Chem.* **277,** 20336–20342
68. Haj, F. G., Markova, B., Klaman, L. D., Bohmer, F. D., and Neel, B. G. (2003) *J. Biol. Chem.* **278,** 739–744

THE JOURNAL OF BIOLOGICAL CHEMISTRY VOL. 281, NO. 43, pp. 32469–32484, October 27, 2006
© 2006 by The American Society for Biochemistry and Molecular Biology, Inc. Printed in the U.S.A.

Calreticulin Represses E-cadherin Gene Expression in Madin-Darby Canine Kidney Cells via Slug*

Received for publication, July 31, 2006 Published, JBC Papers in Press, August 30, 2006, DOI 10.1074/jbc.M607240200

Yasushi Hayashida[‡§1], Yoshishige Urata[‡], Eiji Muroi[‡], Takaaki Kono[‡], Yasuyoshi Miyata[§], Koichiro Nomata[§], Hiroshi Kanetake[§], Takahito Kondo[‡], and Yoshito Ihara[‡¶1,2]

From the [‡]Department of Biochemistry and Molecular Biology in Disease, Atomic Bomb Disease Institute, [§]Department of Urology, Nagasaki University Graduate School of Biomedical Sciences, 1-12-4 Sakamoto, Nagasaki 852-8523, and the [¶]Core Research for Evolutional Science and Technology, Japan Science and Technology Agency, Kawaguchi 332-1102, Japan

Calreticulin (CRT) is a multifunctional Ca^{2+}-binding molecular chaperone in the endoplasmic reticulum. In mammals, the expression level of CRT differs markedly in a variety of organs and tissues, suggesting that CRT plays a specific role in each cell type. In the present study, we focused on CRT functions in the kidney, where overall expression of CRT is quite low, and established CRT-overexpressing kidney epithelial cell-derived Madin-Darby canine kidney cells by gene transfection. We demonstrated that, in CRT-overexpressing cells, the morphology was apparently changed, and the original polarized epithelial cell phenotype was destroyed. Furthermore, CRT-overexpressing cells showed enhanced migration through Matrigel®-coated Boyden chamber wells, compared with controls. E-cadherin expression was significantly suppressed at the protein and transcriptional levels in CRT-overexpressing cells compared with controls. On the other hand, the expression of mesenchymal protein markers, such as N-cadherin and fibronectin, was up-regulated. We also found that the expression of Slug, a repressor of the E-cadherin promoter, was up-regulated by overexpression of CRT through altered Ca^{2+} homeostasis, and this led to enhanced binding of Slug to the E-box element in the E-cadherin promoter. Thus, we conclude that CRT regulates the epithelial-mesenchymal transition-like change of cellular phenotype by modulating the Slug/E-cadherin pathway through altered Ca^{2+} homeostasis in cells, suggesting a novel function of CRT in cell-cell interaction of epithelial cells.

Calreticulin (CRT)[3] is a multifunctional Ca^{2+}-binding molecular chaperone in the endoplasmic reticulum (ER) (1) and known to influence many biological processes, such as the regulation of Ca^{2+} homeostasis (2), intercellular or intracellular signaling (3, 4), gene expression (5), glycoprotein folding (6), and nuclear transport (7). The biological significance of CRT was revealed by the finding that CRT-deficient mice die in the embryonic stage due to impaired development of cardiac and neural tissues (8, 9). CRT is expressed in rat embryos, especially in the heart, but its expression is significantly suppressed after birth (10). On the other hand, CRT-overexpressing transgenic mice are born alive, but suffer a complete heart block and sudden death after birth (11). We also found that overexpression of CRT enhanced sensitivity to apoptosis in myocardial H9c2 cells undergoing differentiation in response to retinoic acid (12) or in cells exposed to stress caused by hydrogen peroxide (13), suggesting the importance of CRT in the pathophysiology of myocardial cells. These findings indicate that CRT expression plays a vital role in the development and physiology of cardiac cells.

Despite its general importance in cell physiology, CRT is differentially expressed in various organs and tissues in mammals, showing a characteristic expression pattern. For example, CRT levels are low in the kidney and heart, compared with the pancreas and liver, in both bovine and rat tissues (14, 15). This characteristic distribution of CRT suggests specific functions in each organ or tissue.

In this study, we focused on the function of CRT in kidney epithelial cells, because CRT levels are quite low in these cells compared with other cell types such as liver cells (14). To investigate the functional effects of CRT overexpression in kidney epithelial cells, we chose Madin-Darby canine kidney (MDCK) cells to establish stable CRT-overexpressing cell lines by gene transfection. MDCK cells are derived from canine kidney and have a well polarized epithelial cell phenotype, maintaining the normal characteristics and functions of renal efferent duct epithelial cells (16). The results showed apparent changes in the morphology of CRT-overexpressing MDCK cells and destruction of the polarized epithelial cell phenotype. Furthermore, overexpression of CRT repressed E-cadherin gene expression through up-regulation of its repressor, Slug, via altered Ca^{2+} homeostasis in MDCK cells. The results suggest a novel function of CRT related to an epithelial-mesenchymal transition-like change of cellular phenotype.

* This work was supported in part by grants-in-aid from the Ministry of Education, Science, Sports, Culture, and Technology of Japan, and fellowship from The Tsukushi Foundation (YH). The costs of publication of this article were defrayed in part by the payment of page charges. This article must therefore be hereby marked "*advertisement*" in accordance with 18 U.S.C. Section 1734 solely to indicate this fact.

[1] Both authors contributed equally to this work.

[2] To whom correspondence should be addressed: Yoshito Ihara, Tel.: +81 95-849-7099; Fax: +81 95-849-7100; E-mail: y-ihara@net.nagasaki-u.ac.jp.

[3] The abbreviations used are: CRT, calreticulin; BAPTA-AM, 1,2-bis(o-aminophenoxy)ethane-*N*,*N*,*N*′,*N*′-tetraacetic acid tetra(acetoxymethyl) ester; BiP, immunoglobulin heavy chain-binding protein; CNX, calnexin; EMSA, electrophoretic mobility shift assay; EMT, epithelial-mesenchymal transition; ER, endoplasmic reticulum; GAPDH, glyceraldehyde-3-phosphate dehydrogenase; MDCK, Madin-Darby canine kidney; PBS, phosphate-buffered saline; RT, reverse transcription; TBS, Tris-buffered saline; TRPV, transient receptor potential vanilloid receptor; EBSS, Earle's balanced salt solution.

EXPERIMENTAL PROCEDURES

Materials—Antibodies against CRT, calnexin (CNX), binding protein (BiP), and ERp57 were purchased from Stressgen (Victoria, BC, Canada). Mouse antibodies against E-cadherin and fibronectin were obtained from BD Biosciences, and rabbit antibodies against β-catenin and pan-cadherin were obtained from Sigma. Antibodies against Slug, SIP1/ZEB2, transient receptor potential vanilloid receptor (TRPV) 5, TRPV6, and polycystin 2 were from Santa Cruz Biotechnology (Santa Cruz, CA). Anti-glyceraldehyde 3-phosphate dehydrogenase (GAPDH) antibody was from Chemicon (Temecula, CA). Anti-Cu,Zn-superoxide dismutase antibody was kindly provided by Dr. K. Suzuki (Hyogo College of Medicine, Japan). Peroxidase-conjugated secondary antibodies against IgG of rabbit, mouse, and goat were from Dako (Glostrup, Denmark). All other reagents used in the study were of high grade and obtained from Sigma and Wako Pure Chemicals (Osaka, Japan).

Cell Lines and Culture—MDCK cells were obtained from American Type Culture Collection (NBL-2). The expression vector for mouse CRT cDNA was constructed as described previously (12). Expression vectors for CRT-gene expression and the control were introduced into MDCK cells using Lipofectamine 2000 reagent (Invitrogen) in accordance with the instructions provided by the manufacturer. Stable gene transfectants were generated after selection with 500 μg/ml G418. Two independent clones expressing high levels of CRT protein were isolated from CRT gene transfectants and used in the study. Cells were cultured in Dulbecco's modified Eagle's medium supplemented with 10% fetal calf serum at 37 °C in an atmosphere of 5% CO_2 and 95% air.

Subcellular Fractionation—Cultured cells were harvested and homogenized with homogenization buffer (10 mM Hepes, pH 7.0, 0.25 M sucrose, 2 mM EGTA, and protease inhibitors (20 μM phenylmethylsulfonyl fluoride, 50 μM pepstatin, and 50 μM leupeptin)) by using a homogenizer of the Potter-Elvehjem type. Subcellular fractionation was performed at 4 °C according to the method of Hogeboom (17) with a modification. The homogenates were centrifuged at 2,000 × *g* for 10 min, and the post-nuclear supernatant was again centrifuged at 8,000 × *g* for 20 min at 4 °C. The post-lysosome supernatant was ultracentrifuged at 55,000 × *g* for 2 h at 4 °C in a Beckman SW41TI rotor (Beckman Instruments). The resulting supernatant contains the soluble cytosolic fraction, and the microsomal pellet represents the ER membrane and lumen proteins as well as Golgi membranes. The pellet was dissolved in lysis buffer (20 mM Tris-HCl (pH 7.2), 130 mM NaCl, and 1% Nonidet P-40, including protease inhibitors), and used as a microsomal fraction.

Immunoblot Analysis—Cells were harvested and lysed in the lysis buffer. The lysate was sonicated on ice for 10 min intermittently, and then solubilized samples were prepared after centrifugation at 10,000 × *g* for 10 min at 4 °C. Protein samples were electrophoresed on 7.5 or 10% SDS-polyacrylamide gels and then transferred onto a nitrocellulose membrane. The membrane was blocked with 5% skim milk in Tris-buffered saline (TBS, 10 mM Tris-HCl (pH 7.5) and 0.15 M NaCl) and incubated at room temperature for 2 h with the primary antibody in TBS containing 0.05% Tween 20. The blots were coupled with peroxidase-conjugated secondary antibodies, washed, and then developed using the ECL detection kit (Amersham Biosciences) according to the instructions recommended by the manufacturer.

Immunofluorescence Microscopy—Cells (5×10^5 per ml) were grown on Lab Tek chamber slides (Nalgen Nunc International, Naperville, IL) for 24 h. They were fixed with 4% paraformaldehyde in phosphate-buffered saline (PBS, pH 7.2) and permeabilized for 10 min with PBS containing 1% Triton X-100. The cells were then blocked with 1% bovine serum albumin in PBS, incubated with the antibody for 1 h, and washed with PBS containing 1% bovine serum albumin. The immunoreactive primary antibodies were visualized with fluorescein isothiocyanate-conjugated anti-rabbit immunoglobulins (Cappel), anti-mouse immunoglobulins (Dako), or rhodamine-conjugated anti-rabbit immunoglobulins (Cappel). After being washed, stained cells were mounted in the Vectashield medium, visualized under a Carl Zeiss LSM5 microscope (Carl Zeiss, Jena, Germany), and analyzed using PASCAL analytic software.

Invasion Assays—A cell invasion assay was carried out using Boyden chambers (Transwell chambers) as described previously (18) with a slight modification. In brief, Transwell chambers, equipped with 8-μm Matrigel®-coated filters (24-well format, BD Biosciences), were rehydrated, and suspensions of 1×10^5 cells in 200 μl of Dulbecco's modified Eagle's medium containing 0.1% fetal calf serum were plated in the upper compartment of the chamber. Serum-free medium (800 μl) was placed in the lower compartment. After 24 h at 37 °C, noninvasive cells on the upper surface of the filters were removed completely by wiping with a cotton swab. The filters were then fixed with 4% paraformaldehyde in PBS and stained with 0.01% crystal violet. Cells on the lower surface were photographed under a microscope (magnification × 100), and enumerated. The data were expressed as the mean ± S.D. of assays performed in triplicate for each filter.

Cell Proliferation Assays—Cell proliferation assays were performed as described previously (12). The proliferation of cultured cells was evaluated by measuring attached live cells photometrically after staining with crystal violet. Cells were seeded onto 96-well plates at a density of 3000 cells per well in 100 μl of medium. After culturing for the times indicated in the text, cells were fixed with 4% paraformaldehyde in PBS, washed three times, and stained with 0.01% crystal violet at room temperature for 20 min. After an extensive wash with water, each well was dried. The stained cells were dissolved in 100 μl of 10% SDS and 0.1 M HCl, and cell numbers were estimated by measuring the absorbance at 570 nm using a microplate reader.

Reverse Transcription-PCR Analysis—Total RNA was isolated from cultured cells (*i.e.* MDCK, NIH3T3, PC3, and LNCaP) or rat tissues using the RNeasy Mini Kit (Qiagen, Hilden, Germany). A specific system for the amplification of mRNA was used: an mRNA-selective PCR kit (AMV, TaKaRa Biomedicals, Shiga, Japan). One microgram of total RNA extracted from cells was used as a template. PCR products were obtained after 30–35 cycles of amplification with an annealing temperature of 55–65 °C. The primer sequences used were as

follows: canine E-cadherin (GenBank™ accession number XM_536807, fragment size 497 bp), forward primer (5′-GGC ATT CTC GGA GGA ATC CTC GC-3′), and reverse primer (5′-CCA TAC ATG TCC GCC AGC TTC-3′); mouse Snail (M95604, 258 bp), forward primer (5′-GGA CTC TCT CCT GGT ACC CCA AGT GCG GCC G-3′), and reverse primer (5′-CCT TGG CCA CCG AGA GCC TGG CCA GCT GC-3′); canine Slug (XM_544069, 454 bp), forward primer (5′-CAG CTC (G/A)GG AGC (G/A)TA CAG CCC C-3′), reverse primer (5′-TAA CCA GGG TCT GGA AAA CGC C-3′); mouse δEF1 (NM011546, 570 bp), forward primer (5′-GCT CCC TGT GCA GTT ACA CCT TTG CAT ACA G-3′), and reverse primer (5′-GCA CCA CAC CCT GAG GAG AAC TGG TTG CCT G-3′); mouse SIP1 (AF033116, 401 bp), forward primer (5′-GCT ACG ACC ATA CCC AGG AC-3′), and reverse primer (5′-TCT CGC CCG AGT GCA GCC-3′); mouse E12/E47 (BC006860, 620 bp), forward primer (5′-AGT GAC CTC CTG GAC TTC AGC ATG ATG TTC CCG CT-3′), and reverse primer (5′-GGG TGC AGG CTG CCA TCT GCC ACG TAG AAG GGG G-3′); human TWIST (BC036704, 436 bp), forward primer (5′-CTG AGC AAC AGC GAG GAA GA-3′), and reverse primer (5′-CTG GTA GAG GAA GTC GAT GT-3′); canis GAPDH (NM_001003142, 979 bp), forward primer (5′-GGT CGG AGT CAA CGG ATT TGG C-3′), and reverse primer (5′-CAT GTA GAC CAT GAG GTC CAC CAC-3′); rat TRPV5 (NM_053787, 411 bp) primer (5′-CCG AGG ATT CCA GAT GCT GGG-3′), and reverse primer (5′-CTC TCC AGC ATC ACT GTG GTG-3′); and rat TRPV6 (NM_053686, 419 bp) primer (5′-GCT CGC CAG ATC CTG GAC CAG-3′), and reverse primer (5′-CGC ATC ACC ATG GTC ACC AGC-3′). The PCR products were subcloned into pCRII (Invitrogen). The nucleotide sequences were confirmed by sequencing with an ALFexpress II system (Amersham Biosciences).

Northern Blot Analysis—The cDNA fragments for E-cadherin, Snail, Slug, δEF1/ZEB1, SIP1/ZEB2, E12/E47, TWIST, and GAPDH generated by RT-PCR were labeled with [α-^{32}P]dCTP (Amersham Biosciences) using a Random Primer DNA Labeling Kit (TaKaRa Biomedicals, Japan). The isolation of cytoplasmic RNA and Northern blotting were essentially performed as described previously (19). Isolated RNAs (10 μg) were electrophoresed on a 1% agarose gel containing 0.6 M formaldehyde, transferred to a nylon membrane, and then hybridized with ^{32}P-labeled probes. Autoradiographed membranes were analyzed using the BAS5000 bioimage analyzer (Fuji Photo Film, Japan).

Electrophoretic Mobility Shift Assays—EMSA for the E-boxes were performed as described previously (19) with a slight modification. Oligonucleotide probes were labeled with [γ-^{32}P]ATP using T4 polynucleotide kinase, and then annealed to double-stranded oligonucleotides. Specific oligonucleotides for E-boxes were prepared according to the nucleotide sequence of the canine E-cadherin gene promoter (GenBank™ accession numbers AF330162 and AF330163). Oligonucleotides used were as follows: E-box A probe, 5′-CCG CCC GCC **GCA GGT** GCA GCC GCA G-3′; E-box B probe, 5′-CTC GCG GCT **CAC CTG** GCG GCC GGA C-3′; and E-box C probe, 5′-GGC GCT GCG **GGC ACC TGT** GAT TC-3′ (bold letters indicate consensus sequences for the E-box). Binding reactions were carried out in 15 μl of reaction mixture (25 mM Tris-HCl (pH 7.0), 6.25 mM $MgCl_2$, 0.5 mM dithiothreitol, and 10% glycerol) containing 10 μg of nuclear extract and 25 ng of labeled oligonucleotides. For the supershift assay, anti-Slug and anti-SIP1 antibodies were added to the reaction mixture during the 30-min binding reaction.

Promoter Reporter Assays—The promoter of human E-cadherin (−178 to +66 bp: GenBank™ accession number L34545) was isolated from the genomic DNA of A549 cells and amplified by PCR using *Pfu* turbo DNA polymerase (Stratagene). The primer sequences used were as follows (20): forward primer (5′-ACT CCA GGC TAG AGG GTC A-3′) and reverse primer (5′-TGG AGC GGG CTG GAG TCT-3′). The PCR product was subcloned into pGL3-Basic vector (KpnI-PstI site, Promega, Madison, WI). PCR-based site-directed mutagenesis was used for the generation of reporter gene constructs with E-box mutations by using a QuikChange site-directed mutagenesis kit (Stratagene), resulting in a mutation in the E-box element from 5′-CANNTG-3′ to 5′-AANNTA-3′ (sense strand). Each vector was transiently transfected into MDCK cells using Lipofectamine 2000 (Invitrogen) as described above. Twenty-four hours after the transfection, luciferase activities were assayed with cellular extracts using a Dual Luciferase Reporter Assay System (Promega) and were normalized to pRL activity.

Assays for Release and Uptake of Ca^{2+} in the Cell—For the $^{45}Ca^{2+}$ release assay, cells were cultured for 48 h with medium containing $^{45}Ca^{2+}$ (1 μCi/ml). After a wash with Ca^{2+}-free Earle's balanced salt solution (EBSS, Invitrogen) containing 3 mM EGTA, cells were detached from the culture plates with trypsinization buffer (0.25% trypsin and 0.02% EDTA in EBSS), and the cell suspensions were preincubated in Ca^{2+}-free EBSS at 37 °C for 3 min, and sequentially stimulated with thapsigargin (0.1 μM), ionomycin (2 μM), and monensin (2 μM). The cell suspensions were collected 5 min after the addition of each reagent and centrifuged. The radioactivity released from the cells was measured in the supernatant. Cell pellets were lysed, and protein amounts were determined using a BCA assay kit (Pierce). $^{45}Ca^{2+}$ release was expressed as the cpm subtracted from those recovered in the preceding collection, and normalized to the protein in the corresponding cell pellets. The uptake of Ca^{2+} was measured radiometrically using the Millipore filtration technique as described previously (13) with a slight modification. The cells were washed with $^{45}Ca^{2+}$ uptake buffer, which consisted of EBSS supplemented with 0.1 mM $CaCl_2$, and cultured for specific periods in $^{45}Ca^{2+}$ uptake buffer containing $^{45}Ca^{2+}$ (5 μCi/ml). Cells were detached from the culture plates by trypsinization buffer, and the cell suspension was filtered through a 0.45-μm nitrocellulose filter (Bio-Rad) under vacuum. The filters were rinsed twice with 0.5 ml of washing buffer (10 mM Hepes (pH 7.4), 150 mM KCl, 2 mM EGTA, and 2.5 mM $MgCl_2$). $^{45}Ca^{2+}$ uptake was calculated by measuring the radioactivity and standardized using protein concentrations.

Measurement of Cytoplasmic-free Ca^{2+}—The cytoplasmic free Ca^{2+} concentration, $[Ca^{2+}]_i$, was measured with a dual-excitation wavelength fluorescence microscope using Fura-2. Cultured cells on quartz-bottom dishes were loaded with 5 μM Fura-2 tetra(acetoxymethyl)ester (Fura-2-AM, Dojindo, Kumamoto, Japan) for 20 min in EBSS with 2 mM $CaCl_2$ in the pres-

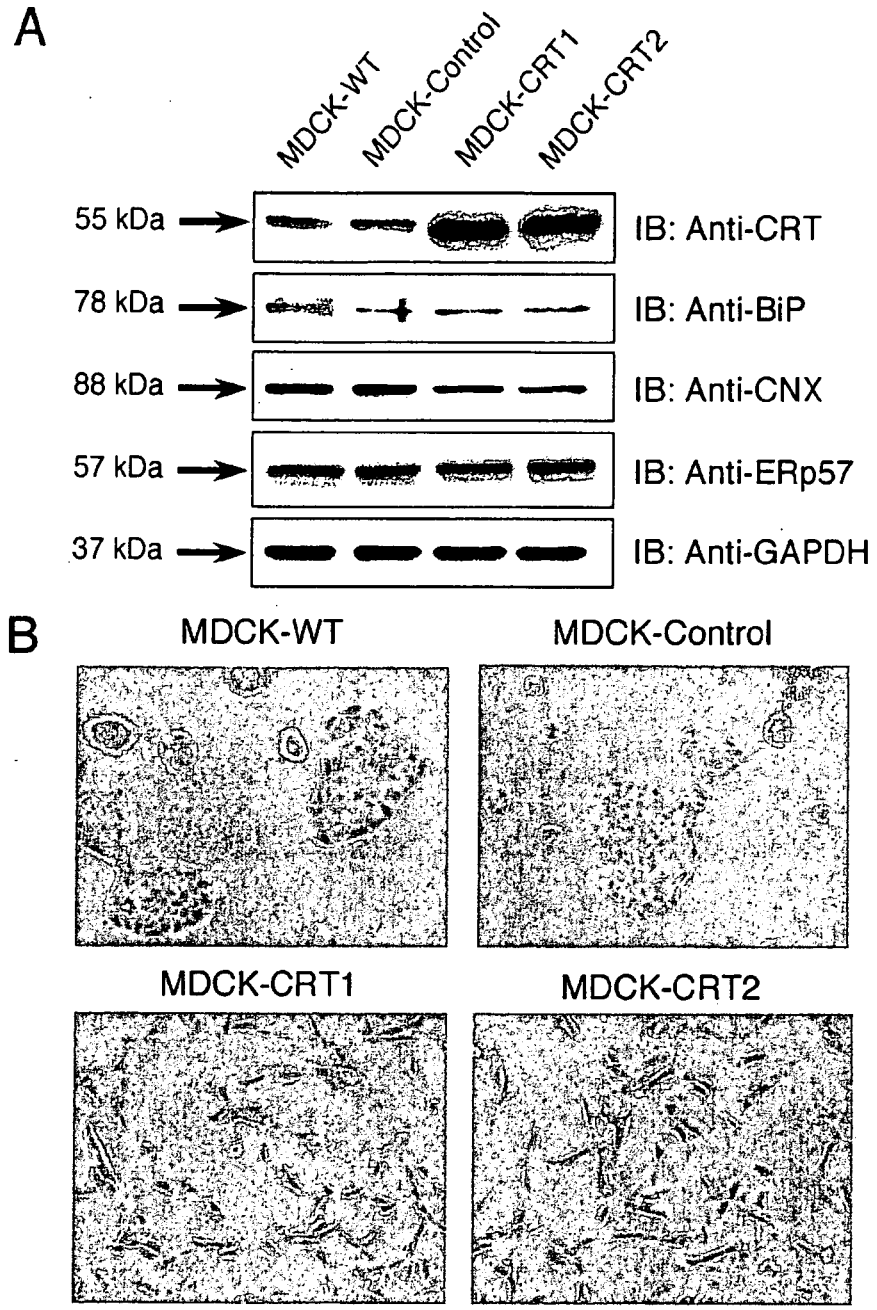

FIGURE 1. **Effect of CRT overexpression on cell morphology in MDCK cells transfected with the CRT gene.** *A*, expression levels of CRT, CNX, BiP, ERp57, and GAPDH were estimated in parental (*MDCK-WT*), mock vector-transfected (*MDCK-Control*), and CRT gene-transfected MDCK (*MDCK-CRT1* and *-CRT2*) cells using immunoblot analysis with specific antibodies as described under "Experimental Procedures." Data represent three independent experiments. *B*, cell morphology of control and CRT gene-transfected cells was examined using phase-contrast microscopy and photographed under a magnification of ×100.

ence of 0.01% pluronic acid F-127. After four washes with EBSS, Fura-2 fluorescence was determined at 37 °C using an IX71 inverted research microscope (Olympus, Tokyo, Japan) and a FURA ratiometric imaging system operating at an emission wavelength of 505 nm with an excitation wavelength of 340 and 380 nm. The FURA ratiometric imaging system includes filters (Chroma Technology Corp., Rockingham, VT) switched by filter wheels (Sutter Instrument Company, Novato, CA) and a MicroMax camera (Roper Scientific, Tucson, AZ) controlled by SlideBook software. To measure the change in $[Ca^{2+}]_i$ during store-operated Ca^{2+} influx, Fura-2-labeled cells were washed with Ca^{2+}-free EBSS, then stimulated with thapsigargin (5 μM) followed by re-addition of Ca^{2+} (2 mM). Stimulated calcium release was calculated as the change in the excitation ratio from baseline integrated over 800 s of stimulation with thapsigargin or Ca^{2+}. The maximal signal (R_{max}) was obtained by adding ionomycin at a final concentration of 4 μM. The minimal signal (R_{min}) was then obtained by adding EGTA at a final concentration of 10 mM, followed by Tris-free base to a final concentration of 30 mM, to increase the pH to 8.3. R is the ratio (F_1/F_2) of the fluorescence of Ex 340 nm, Em 505 nm (F_1) to that of Ex 380 nm, Em 505 nm (F_2). The actual calcium concentration was calculated as $K_d \times (R - R_{min})/(R_{max} - R) \times Sf2/Sb2$ with the K_d equal to 224 nM (21). Sf2/Sb2 is the ratio of Fura-2 fluorescence at 380 nm in Ca^{2+}-free and Ca^{2+}-replete medium, respectively.

RESULTS

Overexpression of CRT Causes Morphological Change in MDCK Cells—Canine renal epithelial MDCK cells were transfected with the expression vector for CRT cDNA to obtain cell lines overexpressing CRT (MDCK-CRT1 and -CRT2). The expression level of CRT was examined by immunoblot analysis in the gene-transfected cells using specific antibodies as described under "Experimental Procedures." Fig. 1*A* shows that the expression of CRT was increased in the overexpressers to ~3-fold the levels in the parental (MDCK-WT) and mock-transfected MDCK (MDCK-Control) cells. The transfection had no apparent effect on the expression of molecular chaperones in the ER, such as BiP, ERp57, and cytosolic GAPDH. However, the expression of CNX, another membrane-bound ER homologue of CRT, showed a slight decrease in the CRT-overexpressing cells. Cell morphology was examined in control and CRT gene-transfected cells by phase-contrast microscopy (Fig. 1*B*). MDCK cells are known to grow in colonies of adherent cells (22, 23). Overexpression of CRT (MDCK-CRT1 and CRT2) caused an apparent morphological change with a fibroblastoid-like

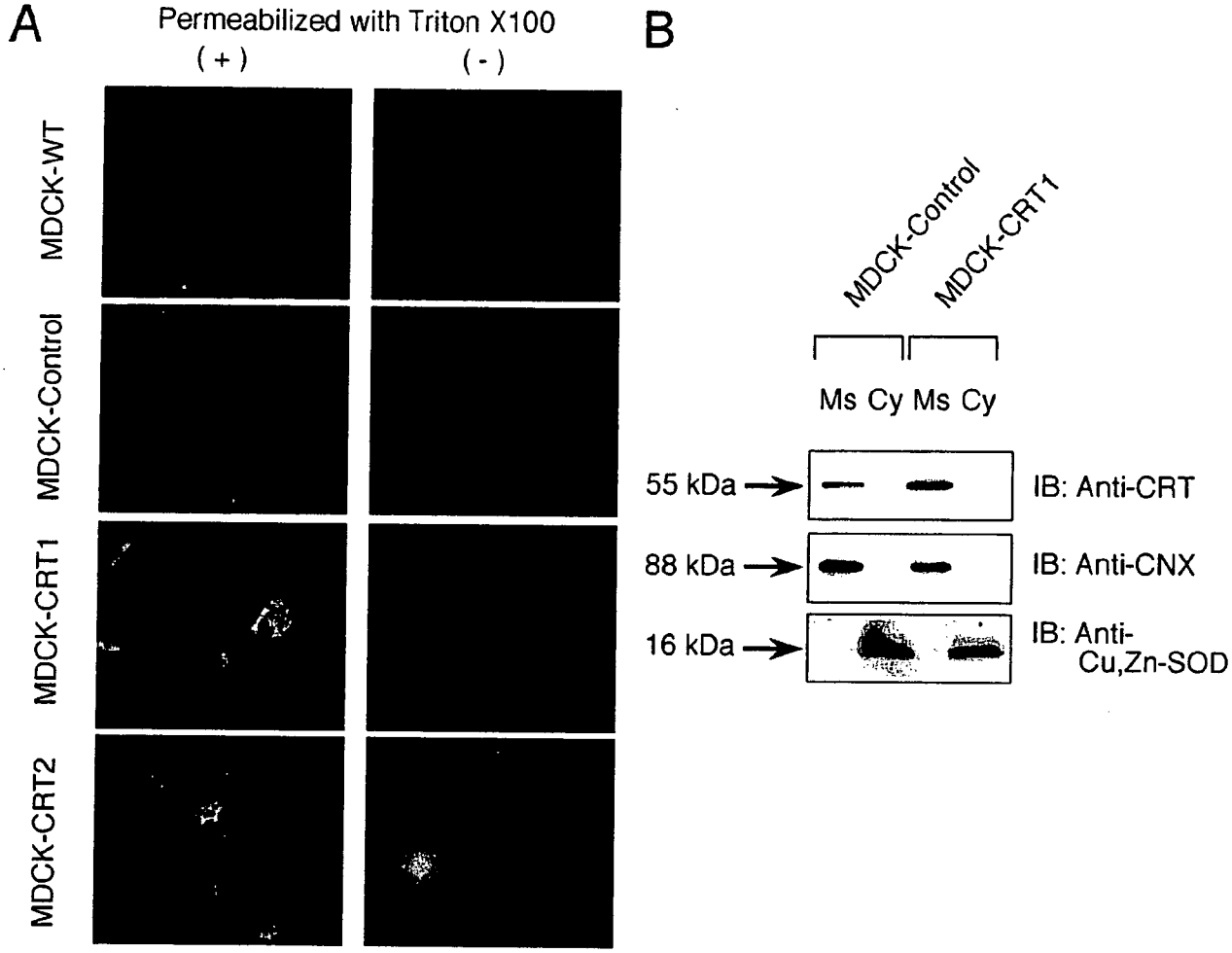

FIGURE 2. *A*, intracellular localization of E-cadherin was evaluated in control and CRT gene-transfected MDCK cells using indirect immunofluorescence microscopy with specific antibodies (magnification, ×200). Data represent three independent experiments. *B*, control and CRT gene-transfected MDCK cells were lysed and fractionated by ultracentrifugation to separate cytosolic and microsomal fractions as described under "Experimental Procedures." The expression of CRT, CNX, and Cu,Zn-superoxide dismutase in each fraction was examined by immunoblot analysis using specific antibodies. *Ms*, microsomes; *Cy*, cytosol. Data represent three independent experiments.

phenotype and loss of cell-cell contacts, although there was no remarkable morphological change in mock-transfected cells compared with parental cells. Intracellular localization of CRT was characterized by immunofluorescence microscopy in control and CRT-overexpressing cells (Fig. 2*A*). Under conditions in which cellular membranes were permeabilized by Triton X-100, strong immunoreactivity for CRT showed a perinuclear localization and a vesicular pattern in CRT-overexpressing cells, although the immunoreactive signal was weak in controls. No significant increase in the cell surface expression of CRT was observed in the CRT-overexpressing cells under conditions without Triton X-100 treatment. To investigate whether the cytosolic localization of CRT was increased in the gene-transfected cells, control and MDCK-CRT1 cells were lysed and fractionated by centrifugation to separate cytosolic and microsomal fractions as described under "Experimental Procedures." As shown in Fig. 2*B*, overexpressed CRT was present in the microsomal but not cytosolic fraction. CNX and Cu,Zn-superoxide dismutase were detected as marker proteins for microsomes and the cytosol, respectively. Similar results were also obtained with MDCK-CRT2 cells (data not shown). Together, these results indicate that overexpression of CRT did not influence the localization of CRT in the ER of MDCK cells.

Overexpression of CRT Enhances Cellular Migration in MDCK Cells—To investigate whether the altered morphology in CRT-overexpressing cells affected cellular functions, a cell invasion assay was performed using a modified Boyden chamber as described under "Experimental Procedures." Cells were seeded on Transwell filters that had been coated with extracellular matrix components, including laminin, fibronectin, and proteoglycans (*i.e.* Matrigel®-coated polycarbonate membrane). After 24 h, the numbers of cells that had migrated through the filters were estimated by enumerating stained cells. There was a significant increase in cell motility through a Matrigel®-coated polycarbonate membrane in CRT-overexpressing cells compared with controls (Fig. 3, *A* and *B*). To investigate whether the enhanced migration of CRT-overexpressing cells was due to an increase in cell growth, cell proliferation was examined in control and CRT gene-transfected cells as described under "Experimental Procedures." However,

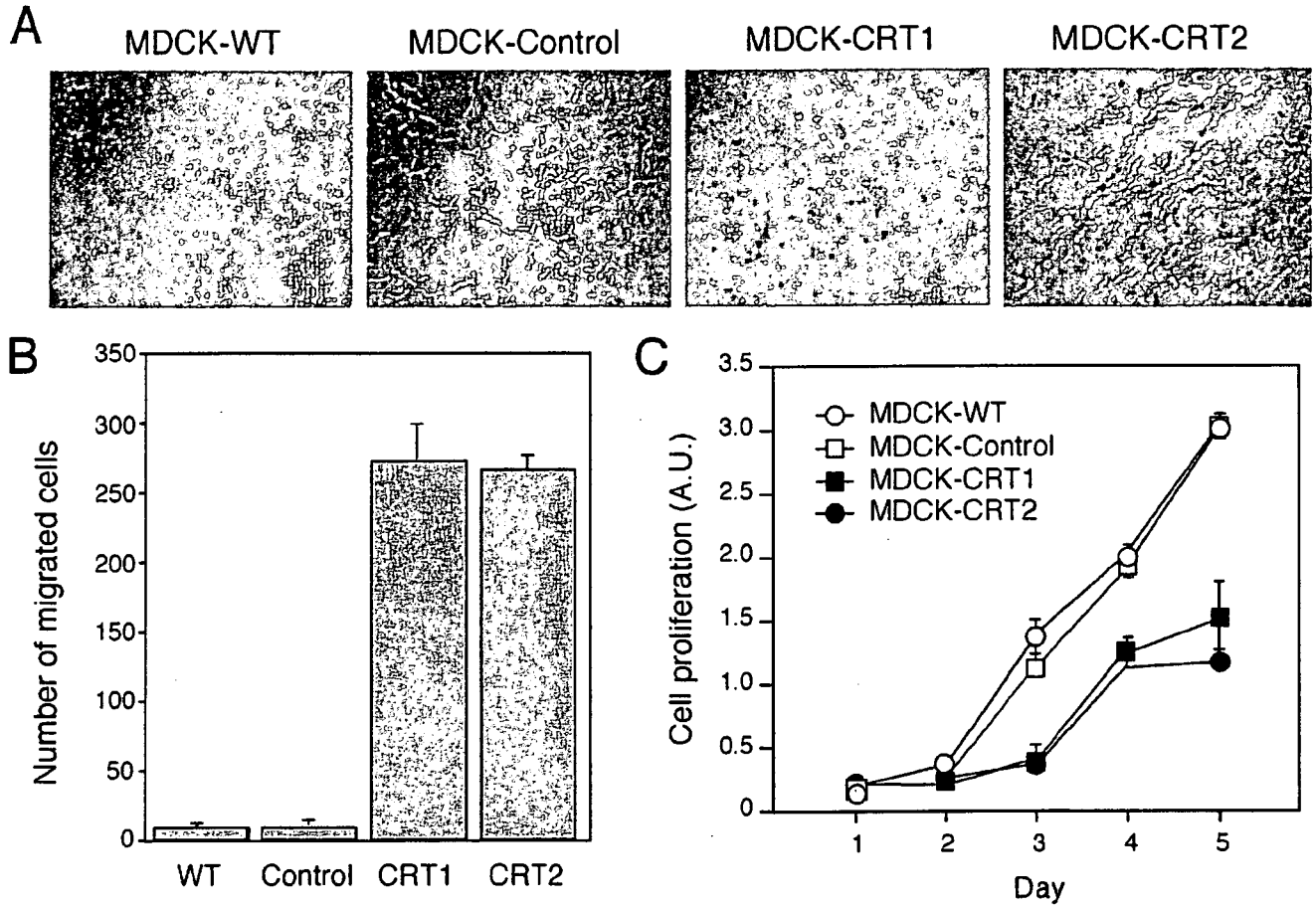

FIGURE 3. **CRT-overexpressing MDCK cells show a migratory phenotype in the Matrigel® invasion assay.** *A*, a cell invasion assay was performed using Boyden chambers, equipped with Matrigel®-coated filters as described under "Experimental Procedures." Suspensions of 1×10^5 cells in Dulbecco's modified Eagle's medium containing 0.1% fetal calf serum were plated in the upper compartment of the chamber. After 24 h of culture, the filters were fixed with 4% paraformaldehyde in PBS and stained with 0.01% crystal violet. Cells on the lower surface were photographed under a microscope (magnification, ×100). *B*, invasion assay was performed as described in *A*, and the number of cells that migrated to the lower surface of filters through the Matrigel® was counted after staining with 0.01% crystal violet and estimated in control and CRT-overexpressing cells. Data represent the mean ± S.D. of three independent experiments. *C*, proliferation of cultured cells was evaluated by measuring attached live cells photometrically after staining with crystal violet as described under "Experimental Procedures." Cells were seeded onto 96-well plates at a density of 3000 cells per well in 100 μl of medium. After culturing for the times indicated in the text, cells were fixed with 4% paraformaldehyde, and stained with 0.01% crystal violet. After a wash, the stained cells were dissolved in 10% SDS and 0.1 M HCl, and then the cell number was estimated by measuring the absorbance at 570 nm using a microplate reader.

the results showed that cell growth was suppressed in CRT-overexpressing cells compared with controls (Fig. 3*C*). These results indicate that the increase in migration of CRT-overexpressing cells was not simply due to an increase in cell growth, implicating other mechanisms related to cell movement, such as cell adhesion and cell de-attachment.

Overexpression of CRT Suppresses E-cadherin Expression—E-cadherin plays an important role in cell-cell interaction in MDCK cells, and a loss of E-cadherin is closely associated with enhanced migration of epithelial cells via a mechanism known as epithelial-mesenchymal transition (EMT) (24). In addition, mesenchymal protein markers (such as N-cadherin and fibronectin) are expressed in EMT (25). To investigate whether overexpression of CRT affected the expression of E-cadherin and EMT-related proteins, an immunoblot analysis was carried out to examine the expression level of EMT-related proteins, such as E-cadherin, N-cadherin, β-catenin, fibronectin, and vinculin, in control and CRT-overexpressing cells (Fig. 4*A*). The results showed that the expression level of E-cadherin was apparently decreased in CRT-overexpressing cells compared with control cells. The expression of β-catenin, a cytoplasmic signaling molecule associated with E-cadherin, was slightly decreased in CRT-overexpressing cells. In contrast, expression of N-cadherin, fibronectin, and vinculin was apparently induced in CRT-overexpressing cells. The intracellular localization of E-cadherin was characterized by immunofluorescence microscopy (Fig. 4*B*). In controls, immunoreactivity for E-cadherin was strong and mainly located at cell-cell contact regions. However, the signal was apparently diminished in CRT-overexpressing cells. These results were consistent with the data from the immunoblot analysis (Fig. 4*A*). Taken together, these results indicate that overexpression of CRT caused a decrease in E-cadherin, and an increase in N-cadherin, fibronectin, and vinculin in MDCK cells, resulting in a gain of migratory characteristics in the cells. This also suggests that CRT expression might be involved in the regulatory mechanism of EMT in the conversion of early stage tumors into invasive malignancies.

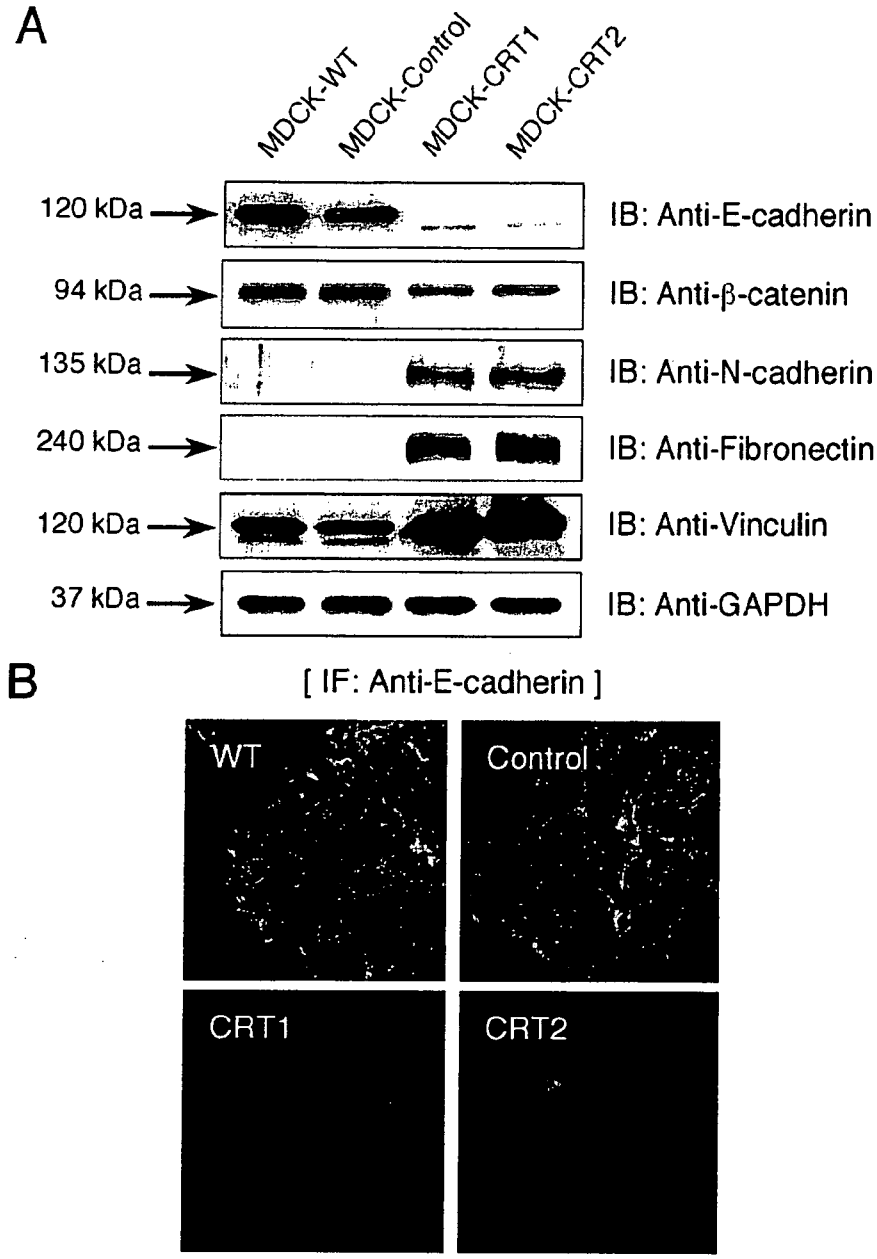

FIGURE 4. *A*, expression levels of E-cadherin, N-cadherin, β-catenin, fibronectin, vinculin, and GAPDH were estimated in control (*MDCK-WT* and *-Control*) and CRT gene-transfected MDCK (*MDCK-CRT1* and *-CRT2*) cells using immunoblot analysis with specific antibodies as described under "Experimental Procedures." Data represent three independent experiments. *B*, intracellular localization of E-cadherin was evaluated in control and CRT gene-transfected MDCK cells using indirect immunofluorescence microscopy with specific antibodies (magnification, ×200). Data represent three independent experiments.

Expression of Slug, a Repressor of the E-cadherin Gene, Is Up-regulated in CRT-overexpressing MDCK Cells—To investigate whether E-cadherin expression is down-regulated in CRT-overexpressing cells at the transcriptional level, we examined the E-cadherin mRNA level by Northern blot analysis in control and CRT-overexpressing cells. As shown in Fig. 5, E-cadherin mRNA expression was definitely reduced in CRT-overexpressing cells. The expression of the E-cadherin gene is known to be regulated by several transcriptional repressors, including Snail, Slug, δEF1/ZEB1, SIP1/ZEB2, E12/E47, and Twist (25–27). To investigate whether some of the repressors are involved in regulating the suppression of E-cadherin gene expression, the mRNA levels of the repressors were examined by Northern blot analysis using specific probes as described under "Experimental Procedures." As shown in Fig. 5, the expression of Slug mRNA was apparently up-regulated in CRT-overexpressing cells. The level of SIP1 mRNA was also slightly increased in the gene-transfected cells compared with the controls. On the other hand, there was little deference in the expression levels of Snail and Twist and no expression of δEF1 and E12/E47 in control and CRT-overexpressing cells. Therefore, we focused on the functions of Slug and SIP1 in the mechanism of E-cadherin gene suppression in CRT-overexpressing cells.

Slug Binds to the E-box Element in the E-cadherin Gene Promoter to Repress Gene Expression in CRT-overexpressing MDCK Cells—Slug and SIP1 block E-cadherin transcription by binding to specific DNA sequences (5′-CANNTG) called E-boxes (27). As shown in Fig. 6*A*, in the canine E-cadherin gene promoter, there are two E-box sites located from −78 to −73 (designated as E-box A) and from −28 to −23 (designated as E-box B), and downstream of the transcription start site there is another 5′-CANNTG sequence positioned from +22 to +27 (designated as E-box C) (23, 28, 29). To investigate whether Slug or SIP1 could interact with E-boxes in the E-cadherin gene promoter, EMSA was performed with nuclear extracts from control (MDCK-Control) and CRT-overexpressing (MDCK-CRT1) cells using ^{32}P-labeled oligonucleotides designed for each E-box (Fig. 6*B*). In the case of E-box A, a major band appeared with the extracts from MDCK-CRT1 cells but not with extracts from controls. The shifted band was not affected by the presence of antibodies against Slug and SIP1, suggesting that Slug and SIP1 had no correlation with E-cadherin gene repression. In the case of E-box B, a major band also appeared with extracts from MDCK-CRT1 cells but not with control extracts. The shifted band was not affected by the anti-SIP1 antibody but disappeared with addition of the anti-Slug antibody, suggesting that Slug was involved in repression of the E-cadherin gene in MDCK-CRT1 cells. In the case of

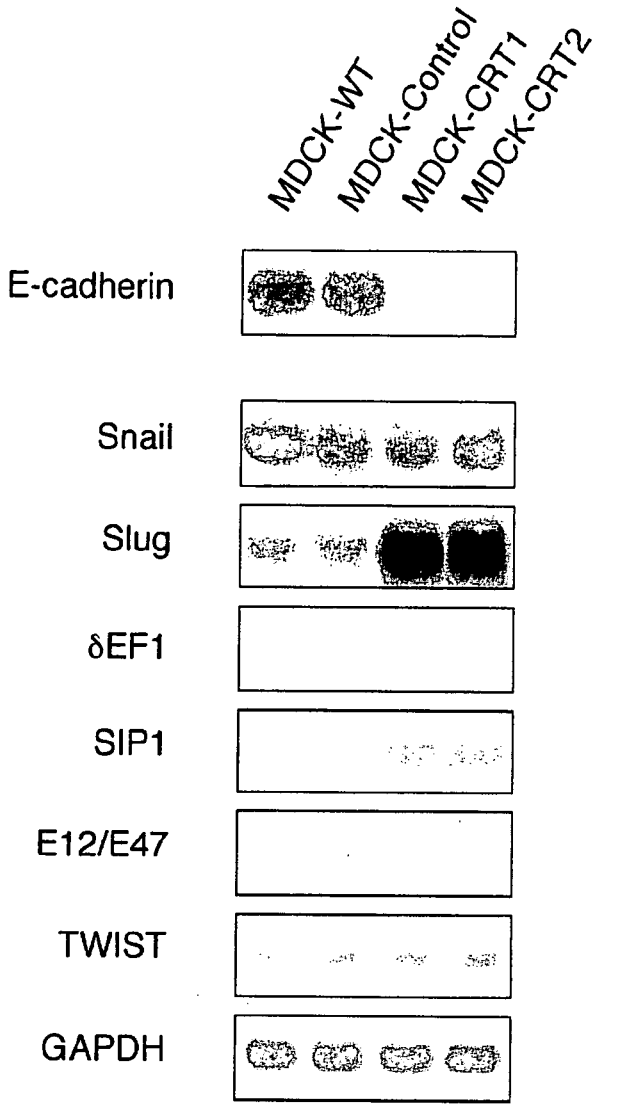

FIGURE 5. **Northern blot analysis was carried out for E-cadherin and transcriptional repressors of the E-cadherin gene in control and CRT-overexpressing MDCK cells.** Northern blot analysis was carried out in control (*MDCK-WT* and *-Control*) and CRT gene-transfected MDCK (*MDCK-CRT1* and *-CRT2*) cells. Specific oligonucleotide probes for E-cadherin, Snail, Slug, δEF1, SIP1, E12/E47, TWIST, and GAPDH were prepared and used for the assay as described under "Experimental Procedures."

E-box C, no shifted band appeared in either control or MDCK-CRT1 cells, suggesting that E-box C was not involved in the regulation of E-cadherin. The shifted bands completely disappeared when a 500-fold excess of unlabeled oligonucleotide probes was added. Similar results were also obtained with MDCK-CRT2 cells (data not shown). Taken together, these results indicate that, in CRT-overexpressing cells, the DNA-protein interactions are enhanced in E-box A and B in the E-cadherin promoter, and that Slug specifically interacts with E-box B, implicating Slug in E-cadherin gene repression by overexpression of CRT. Next, to elucidate whether the binding of Slug to E-box B in the E-cadherin promoter was linked to the transcriptional activation of E-cadherin, we examined the E-cadherin promoter activity in control and CRT-overexpressing cells using a luciferase reporter plasmid, in which a proximal E-cadherin promoter fragment containing E-boxes A, B, and C is connected upstream of the luciferase gene. To investigate the importance of E-boxes in the transcriptional repression, a mutation was generated in E-boxes A and B (from 5′-CANNTG to 5′-AANNTA) as described under "Experimental Procedures" (Fig. 6*C*). The activity of luciferase was assayed with the cells transfected with each vector. As shown in Fig. 6*D*, in MDCK-CRT1 cells, the promoter activity was suppressed to ~50% of the control level. The repression of promoter activity in MDCK-CRT1 cells was apparently restored by mutation of E-box B, but not by mutation of E-box A. Similar results were also obtained with MDCK-CRT2 cells (data not shown). These results suggest that E-box B plays the most significant role in the repression of E-cadherin gene transcription in CRT-overexpressing cells.

Ca^{2+} Homeostasis Is Altered in CRT-overexpressing MDCK Cells—In previous reports, overexpression of CRT led to an increase in the intracellular store of Ca^{2+} (1). CRT also appears to modulate store-operated Ca^{2+} influx (1, 30). We also reported that overexpression of CRT influences Ca^{2+} homeostasis in myocardial H9c2 cells under various stressful conditions (12, 13). However, the mechanism by which overexpression of CRT influenced Ca^{2+} homeostasis was not clear in MDCK cells. To investigate whether the intracellular store of Ca^{2+} was affected by overexpression of CRT, intracellular Ca^{2+} pools were characterized in control and CRT-overexpressing cells. After 48 h of loading with $^{45}Ca^{2+}$, the cells were washed and resuspended in Ca^{2+}-free buffer. Unidirectional fluxes to the extracellular medium after stimulation with several Ca^{2+} modulators were then measured as described under "Experimental Procedures." Thapsigargin (an inhibitor of sarcoplasmic/endoplasmic reticulum Ca^{2+}-ATPase), ionomycin (a Ca^{2+} ionophore), and monensin (another ionophore affecting acidic stores) were used to stimulate the cellular Ca^{2+} pools (Fig. 7*A*). The results showed that cellular Ca^{2+} levels were apparently increased mainly in the thapsigargin-sensitive Ca^{2+} pools of CRT-overexpressing cells, compared with controls, suggesting that Ca^{2+} stores in the ER were increased in CRT-overexpressing cells.

Next, to investigate whether the intracellular Ca^{2+} homeostasis was affected by overexpression of CRT, the cytoplasmic free Ca^{2+} concentration ($[Ca^{2+}]_i$) and response of $[Ca^{2+}]_i$ to thapsigargin were examined in control and CRT-overexpressing cells using Fura2-AM as described under "Experimental Procedures." The release of Ca^{2+} from ER stores by thapsigargin was measured in the absence of extracellular Ca^{2+}, and the influx of Ca^{2+} from the extracellular space was measured by re-adding Ca^{2+} to the external medium. As shown in Fig. 7 (*B* and *C*), the basal level of $[Ca^{2+}]_i$ was slightly increased in CRT-overexpressing cells, compared with controls. Thapsigargin induced a greater increase of $[Ca^{2+}]_i$ in CRT-overexpressing cells than in the controls, indicating that substantially more Ca^{2+} was released from Ca^{2+} stores in CRT-overexpressing cells. Furthermore, the Ca^{2+} influx-induced increase of $[Ca^{2+}]_i$ when Ca^{2+} was re-added was also more extensive in CRT-overexpressing cells than the controls. These results suggest that the level of $[Ca^{2+}]_i$ was relatively high in CRT-overexpressing cells compared with controls. However, it was reported that store-

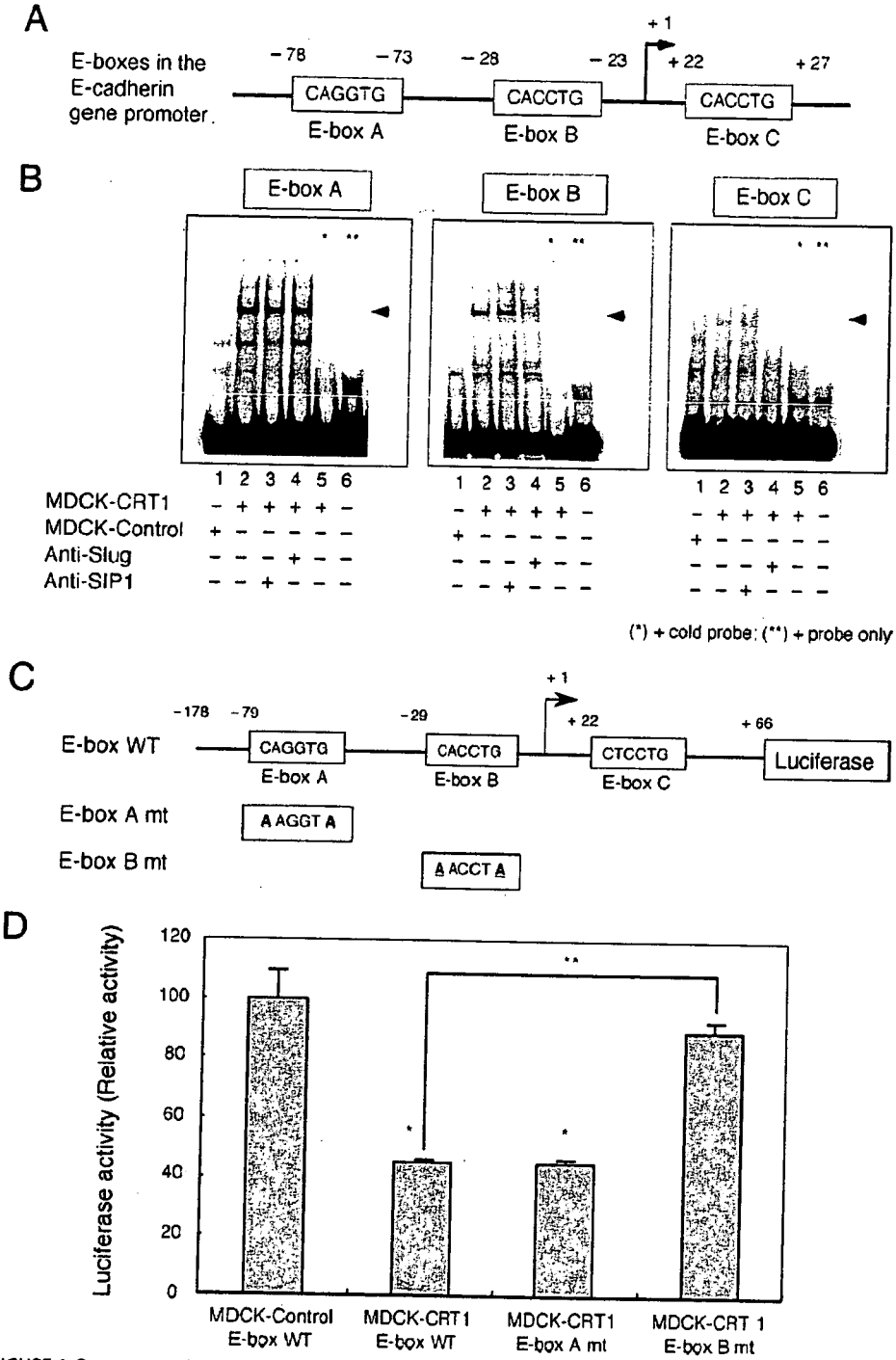

FIGURE 6. **Overexpression of CRT represses E-cadherin gene expression via the binding of Slug to E-box B in the gene promoter of E-cadherin.** *A*, schematic representation of proximal E-box elements (*E-boxes A–C*) in the canine E-cadherin gene promoter. *B*, EMSAs were carried out as described under "Experimental Procedures" using oligonucleotide probes for E-boxes A–C. In *lane 1*, nuclear extracts of MDCK-Control cells were incubated with ^{32}P-labeled probes. From *lane 2* to *lane 4*, nuclear extracts of MDCK-CRT1 cells were incubated with ^{32}P-labeled probes. In *lane 3*, anti-SIP1 antibody was added to the reaction mixture during the binding reaction. In *lane 4*, anti-Slug antibody was added to the reaction mixture. In *lane 5*, nuclear extracts of MDCK-CRT1 cells were incubated with ^{32}P-labeled probes and a 500-fold excess of the unlabeled probes. In *lane 6*, ^{32}P-labeled probes were loaded without nuclear extracts. *Arrowheads* indicate shifted bands of protein complex with ^{32}P-labeled probes. *C*, schematic representation of proximal E-box elements mutated at E-boxes A and B. In E-box A, the sequence of CAGGTG was changed to AAGGTA. In E-box B, the sequence of CACCTG was changed to AACCTA. *D*, MDCK-Control or MDCK-CRT1 cells were transiently transfected with various luciferase gene fusion plasmids with the E-cadherin gene promoter with (*E-boxes A mt* and *B mt*) or without (*E-box WT*) mutations. Luciferase activity was then assayed as described under "Experimental Procedures." Each value represents the mean ± S.D. of at least three experiments. *, $p < 0.01$ *versus* MDCK-Control cells with E-box WT; **, $p < 0.01$ *versus* MDCK-CRT1 cells with E-box B mt.

operated Ca^{2+} entry was suppressed by overexpression of CRT in several cell types (30) and was inconsistent with the present results of CRT-overexpressing MDCK cells.

To further investigate why the influx of Ca^{2+} was enhanced in CRT-overexpressing cells, we examined the expression of epithelial Ca^{2+} channels in control and CRT-overexpressing cells. In Fig. 8*A*, the expression of epithelial Ca^{2+} channels related to cellular Ca^{2+} uptake, such as TRPV5, TRPV6 (31), and polycystin 2 (32), was examined by immunoblot analysis using specific antibodies in control and CRT-overexpressing cells. The expression of TRPV5 was stronger in the CRT-overexpressing cells. In contrast, TRPV6 was not detected in either of the cells. Polycystin 2 was similarly expressed in both control and CRT-overexpressing cells. In Fig. 8*B*, the expression of TRPV5 was also examined by immunofluorescence microscopy. The immunoreactive signals for TRPV5 showed a perinuclear vesicular distribution and were abundant in CRT-overexpressing cells compared with less signals in control cells. In Fig. 8*C*, transcriptional levels of TRPV5 and -6 were examined in control and CRT-overexpressing cells by RT-PCR using specific primers as described under "Experimental Procedures." The results showed that the transcriptional expression of TRPV5 was detected in CRT-overexpressing cells but not in control cells under the experimental conditions. The expression of TRPV6 was not detected in either control or CRT-overexpressing cells. For positive controls, RNAs from rat kidney and prostate were used for RT-PCR to detect TRPV5 and -6, respectively (33). Together, these results indicate that the expression of TRPV5 is apparently up-regulated in CRT-overexpressing cells compared with controls, suggesting a functional link with the up-regulation of Ca^{2+} influx in

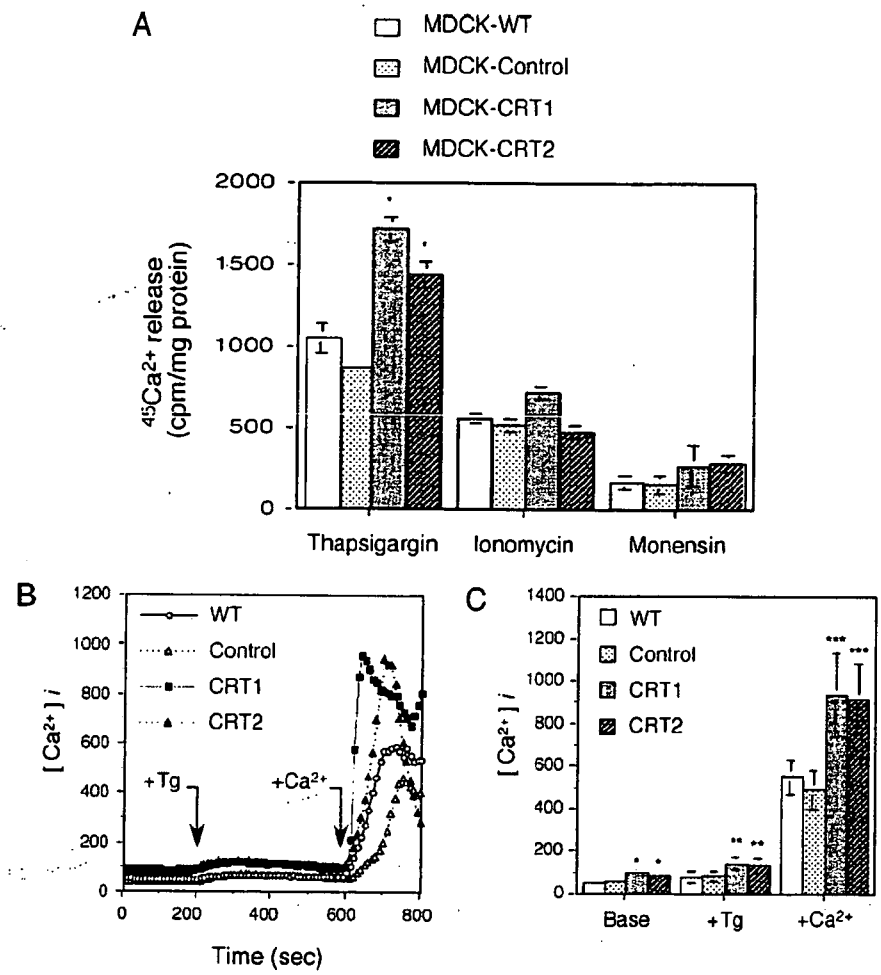

FIGURE 7. **Effect of CRT overexpression on intracellular Ca^{2+} pools and store-operated Ca^{2+} influx in MDCK cells.** *A*, control (*MDCK-WT* and *-Control*) and CRT-overexpressing (*MDCK-CRT1* and *-CRT2*) cells were cultured with $^{45}Ca^{2+}$ (1 μCi/ml) for 48 h, then detached from the culture dish and resuspended in Ca^{2+}-free EBSS. Cell suspensions were preincubated at 37 °C for 3 min, and sequentially stimulated with thapsigargin (0.1 μM), ionomycin (2 μM), and monensin (2 μM). The cell suspensions were collected 5 min after the addition of each reagent, and centrifuged. The radioactivity released from the cells was measured in the supernatant. Cell pellets were lysed, and protein amounts were determined using a BCA assay kit (Pierce). Each value represents the mean ± S.D. of the cpm subtracted from those recovered in the preceding collection, and normalized to the protein in the corresponding cell pellets. *, $p < 0.01$ *versus* MDCK-WT or MDCK-Control cells treated with thapsigargin. *B*, control and CRT-overexpressing cells were loaded with Fura-2-AM, and washed with Ca^{2+}-free medium. The cells were stimulated with thapsigargin (5 μM) followed by Ca^{2+} (2 mM). $[Ca^{2+}]_i$ was monitored by measuring Fura-2 fluorescence as described under "Experimental Procedures." *C*, mean values of $[Ca^{2+}]_i$ measured in control and CRT-overexpressing cells during sore-operated Ca^{2+} influx are shown. Each value represents the mean ± S.D. of at least six experiments. *, $p < 0.01$ *versus* MDCK-WT or MDCK-Control cells; **, $p < 0.01$ *versus* MDCK-WT or MDCK-Control cells treated with thapsigargin (5 μM); ***, $p < 0.01$ *versus* MDCK-WT or MDCK-Control cells treated with Ca^{2+} (2 mM).

CRT-overexpressing cells. To investigate whether the basal level of Ca^{2+} influx was affected in CRT-overexpressing cells, $^{45}Ca^{2+}$ uptake was examined in control and CRT-overexpressing cells as described under "Experimental Procedures." As shown in Fig. 8*D*, the uptake of $^{45}Ca^{2+}$ was enhanced in CRT-overexpressing cells, compared with controls. This seems to be compatible with the up-regulated expression of TRPV5 in CRT-overexpressing cells. Collectively, these results indicate that intracellular Ca^{2+} homeostasis is apparently altered by overexpressed CRT in MDCK cells, and this may lead to sustained up-regulation of $[Ca^{2+}]_i$ in the cells.

Overexpression of CRT Down-regulates E-cadherin Gene Expression through Alteration of Ca^{2+} Homeostasis—To determine whether the increase in $[Ca^{2+}]_i$ was part of the causative mechanism for E-cadherin gene repression in the gene-transfected cells, E-cadherin expression was examined in control cells treated with thapsigargin (5 μM) or ionomycin (1 μM) to increase $[Ca^{2+}]_i$. RT-PCR analysis was performed to examine E-cadherin expression at the mRNA level. As shown in Fig. 9*A*, the mRNA levels of E-cadherin were decreased in both cases with thapsigargin and ionomycin in a time-dependent manner. The expression of E-cadherin was also examined by immunofluorescence microscopy after a 4-h treatment with thapsigargin or ionomycin (Fig. 9*B*). The results showed that the immunoreactive signal for E-cadherin was diminished in both cases with thapsigargin and ionomycin, compared with untreated controls. To investigate further the effect of increased $[Ca^{2+}]_i$ on the repressors of the E-cadherin gene, we examined mRNA levels of Slug by RT-PCR analysis in control cells treated with or without thapsigargin or ionomycin for 1 h. Expression of Slug was increased in both cases with thapsigargin and ionomycin, compared with untreated controls (Fig. 9*C*). The expression of Slug was also examined by immunofluorescence microscopy in control cells after 4 h of treatment with thapsigargin or ionomycin (Fig. 9*D*). The results showed that the immunoreactive signal for Slug was increased in both cases with thapsigargin and ionomycin, compared with untreated controls. In the cells treated with thapsigargin or ionomycin, increased signals for Slug were detected in the cytoplasm and nucleus and were similar with the signals in the CRT-overexpressing cells (MDCK-CRT1). Taken together, these results indicate that the rise in $[Ca^{2+}]_i$ increased the expression of Slug and decreased the expression of E-cadherin, suggesting a Ca^{2+}-dependent repression of E-cadherin through Slug in MDCK cells.

Next, to further investigate whether the repression was caused by an rise in $[Ca^{2+}]_i$ in CRT-overexpressing cells, the effect of BAPTA-AM, a cell-permeable Ca^{2+} chelator that reduces intracellular Ca^{2+} levels, on the expression of E-cad-

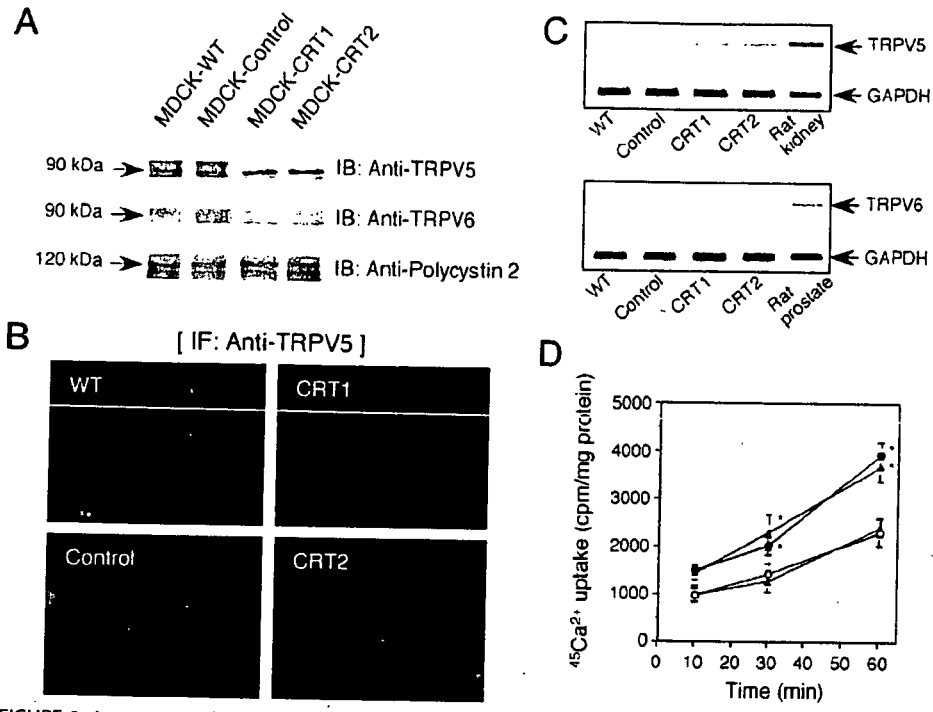

FIGURE 8. *A*, expression levels of TRPV5, TRPV6, and polycystin 2 were estimated in control (*MDCK-WT* and *-Control*) and CRT-overexpressing (*MDCK-CRT1* and *-CRT2*) cells using immunoblot analysis with specific antibodies as described under "Experimental Procedures." *B*, intracellular localization of TRPV5 was evaluated in control and CRT gene-transfected MDCK cells using indirect immunofluorescence microscopy with specific antibodies (magnification, ×200). Data represent three independent experiments. *C*, mRNA expression of TRPV5, TRPV6, and GAPDH was examined in control and CRT-overexpressing cells by RT-PCR analysis using specific primers. *D*, control and CRT-overexpressing cells were washed with EBSS, and then cultured for indicated periods in $^{45}Ca^{2+}$ uptake buffer containing $^{45}Ca^{2+}$ (5 μCi/ml) as described under "Experimental Procedures." After a wash with EBSS, the cells were harvested and $^{45}Ca^{2+}$ uptake was measured. *Open triangle*, MDCK-WT; *open circle*, MDCK-Control; *closed triangle*, MDCK-CRT1; *closed circle*, MDCK-CRT2. Each value represents the mean ± S.D. of three independent experiments. *, $p < 0.01$ *versus* MDCK-WT or MDCK-Control cells at corresponding times.

herin or Slug was examined in MDCK-CRT1. RT-PCR analysis was performed to examine E-cadherin expression at the mRNA level. As shown in Fig. 10*A*, the mRNA levels of E-cadherin were increased by BAPTA-AM (10 μM) in a time-dependent manner. The expression of E-cadherin was also examined by immunofluorescence microscopy after 8 h of treatment with BAPTA-AM (Fig. 10*B*). The results showed that the immunoreactive signal for E-cadherin was increased by BAPTA-AM, compared with untreated MDCK-CRT1. Similar results were also obtained with MDCK-CRT2 cells (data not shown). To investigate further the effect of decreased $[Ca^{2+}]_i$ on the repressors of the E-cadherin gene, we examined mRNA levels of Slug by RT-PCR analysis in MDCK-CRT1 cells treated with BAPTA-AM. Expression of Slug was decreased by BAPTA-AM, compared with untreated MDCK-CRT1 cells (Fig. 10*C*). The expression of Slug was also examined by immunofluorescence microscopy in the gene-transfected cells after 8 h of treatment with BAPTA-AM (Fig. 10*D*). The results showed that the immunoreactive signal for Slug was decreased by BAPTA-AM, compared with untreated MDCK-CRT1 cells. Similar results were also obtained with MDCK-CRT2 cells (data not shown). Taken together, these results indicate that a drop in $[Ca^{2+}]_i$ decreased the expression of Slug and increased the expression of E-cadherin. They also suggest a Ca^{2+}-dependent repression of E-cadherin through Slug in CRT-overexpressing cells.

In addition, the binding ability of E-box elements of the E-cadherin promoter was also examined by EMSA in control cells treated with or without thapsigargin (5 μM) or ionomycin (1 μM) for 2 h (Fig. 11*A*). The results showed that a positive gel-shift band appeared in response to the treatment with both thapsigargin and ionomycin in the case of E-box B, but not E-boxes A or C. The gel-shift band induced by thapsigargin or ionomycin was similar to that seen in the case of nuclear extracts from CRT-overexpressing cells (MDCK-CRT1). Next, to confirm the Ca^{2+}-dependent up-regulation of E-cadherin gene expression, CRT-overexpressing cells were treated for 2 h with BAPTA-AM (10 μM), and then the binding ability of E-box elements of the E-cadherin promoter was examined by EMSA (Fig. 11*B*). The results showed that the protein-binding ability of E-box B apparently decreased in MDCK-CRT1 cells treated with BAPTA-AM, although that of E-box A also slightly decreased with BAPTA-AM. There was no influence of BAPTA-AM on the binding ability of E-box C. Similar results were also obtained with MDCK-CRT2 cells (data not shown). Taken together, these results indicate that overexpression of CRT in MDCK cells causes an increase in $[Ca^{2+}]_i$, which up-regulates Slug expression, resulting in suppression of E-cadherin gene expression via E-box B in the gene promoter.

DISCUSSION

In this study, we have shown that overexpression of CRT repressed E-cadherin gene expression in MDCK cells, leading to alteration of cell characteristics such as morphology and motility. E-cadherin, a Ca^{2+}-dependent transmembrane glycoprotein, plays a key role in the maintenance of intercellular adhesion, regulation of tissue morphogenesis, and cell polarity in epithelial cells, and disruption of E-cadherin expression or function causes invasion and metastasis (34–37). Therefore, E-cadherin is thought to be an invasion suppresser (38, 39). E-cadherin-mediated cell-cell adhesion plays a critical role in early embryonic development through a mechanism known as EMT (24). EMT also determines progression in epithelial tumors, occurring concomitantly with the acquisition of migratory properties followed by down-regulation of E-cadherin expression (40, 41). In CRT-overexpressing MDCK cells, the morphology changed from a polarized, epithelial phenotype to a highly motile fibroblastoid-like, mesenchymal phenotype. In addition to a decrease in E-cadherin expression, the expression level of mesenchymal markers, such as N-cadherin and

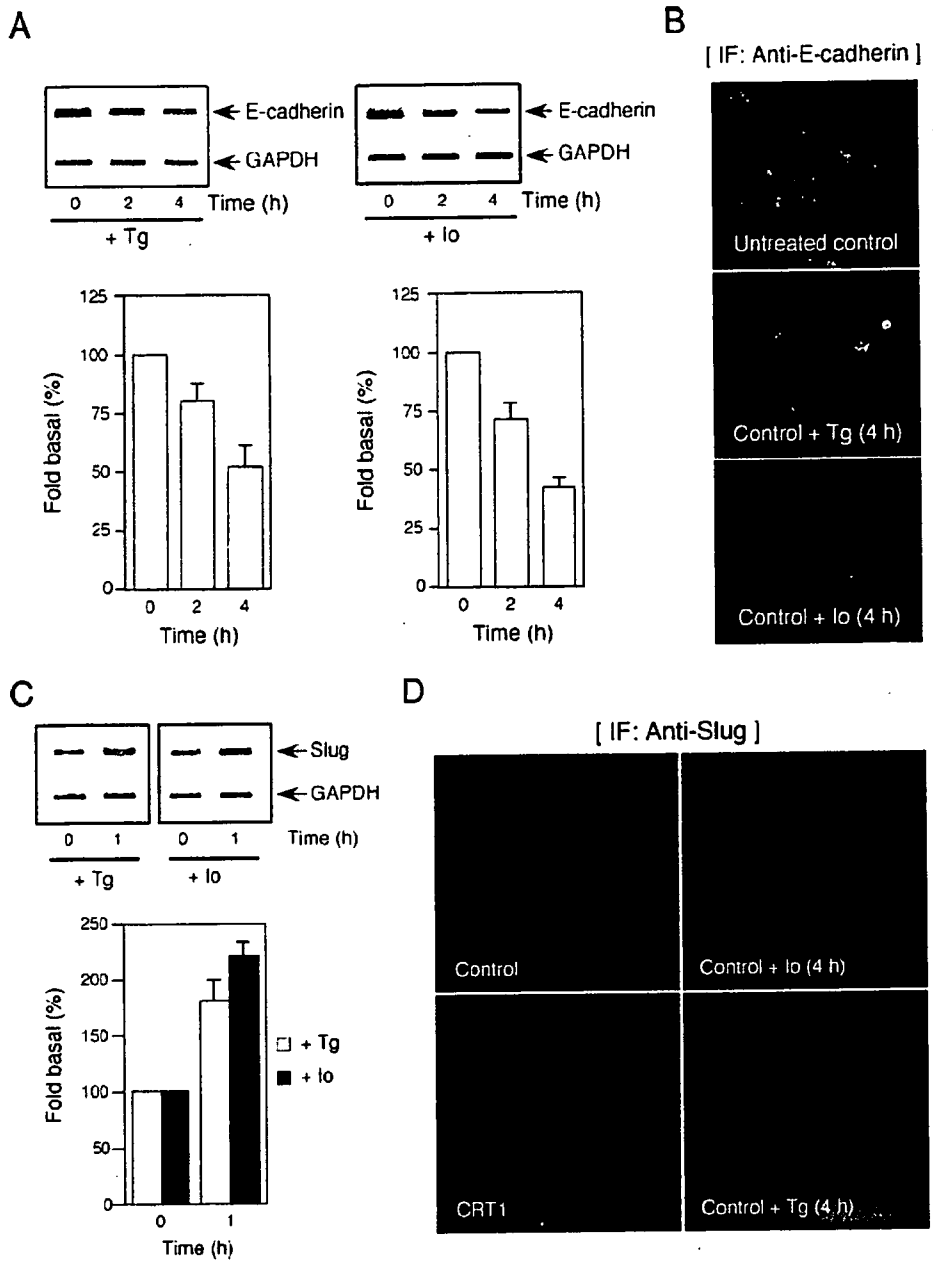

FIGURE 9. **Ca^{2+} modulators of thapsigargin and ionomycin suppressed the expression of E-cadherin and up-regulated the expression of Slug in MDCK cells.** *A*, control cells were treated with thapsigargin (*Tg*, 5 μM) or ionomycin (*Io*, 1 μM) for the periods indicated, and the level of E-cadherin expression was examined by RT-PCR analysis using specific primers. *B*, control cells were treated for 4 h with thapsigargin or ionomycin as described in *A*, and the expression of E-cadherin was examined by immunofluorescence microscopy by using the anti-E-cadherin antibody. Data represent three independent experiments. *C*, control cells were treated with thapsigargin (*Tg*, 5 μM) or ionomycin (*Io*, 1 μM) for 1 h, and the level of Slug expression was examined by RT-PCR analysis using specific primers. *D*, control cells were treated for 4 h with thapsigargin or ionomycin as described in *A*, and the expression of Slug examined by immunofluorescence microscopy by using the anti-Slug antibody. The immunofluorescence of Slug was also shown in CRT-overexpressing (MDCK-CRT1) cells. Data represent at least three independent experiments.

fibronectin, was apparently up-regulated in the gene-transfected cells. The conversion of the cadherin class is observed in EMT in general (42–44). These results strongly suggest that overexpression of CRT could cause EMT-like changes in MDCK cells.

Recently, it has been reported that EMT is caused by several transcriptional repressors of E-cadherin, such as the zinc finger factors (*i.e.* Snail (22, 23), Slug (45, 46), δEF1/ZEB1 (47, 48), and SIP1/ZEB2 (28, 49)) and the basic helix-loop-helix factors (*i.e.* E12/E47 (27, 50) and Twist (51, 52)). The zinc finger factors have been described to directly repress transcription of the E-cadherin gene by binding to E-boxes (consisting of the sequence 5′-CANNTG) in the proximal E-cadherin promoter (23, 28, 29, 53), and E-boxes are the recognition sites of the basic helix-loop-helix family (54). Bolos *et al.* (46) reported that stable expression of Slug in MDCK cells leads to full repression of E-cadherin at the transcriptional level and triggers a complete EMT, although the binding affinity of Slug to the E-box is lower than that of Snail and E12/E47. Slug is also responsible for repression of the E-cadherin gene through binding to E-box C in human breast cancer cells (29). On the other hand, Snail is also a repressor of E-cadherin expression in various epithelial tumor cells (23). In SIP1-expressing human mammary cancer cells, mutation of E-box B (designated as E2-box 3) restored the E-cadherin promoter activity similarly to mutation of E-Box A (designated as E2-box1) (28). These studies indicate that the regulatory system for repression of the E-cadherin gene is complex, suggesting that the specific repressors could work in a cell type-dependent manner (29). In this study, we showed that overexpression of CRT induced the expression of Slug and that this enhanced the binding of Slug to E-box B in the E-cadherin gene promoter to repress E-cadherin expression in MDCK cells.

In addition to transcriptional repression, several molecular mechanisms that down-regulate E-cadherin function have been reported, including gene mutation (55), promoter methylation (56), and post-translational modification of the cadherin-catenin complex (57). Indeed, we observed that, in CRT-overexpressing cells, the promoter activity of E-cadherin was suppressed to ~50% of the control level, despite extensive suppression of E-cadherin gene expression. Therefore, other regulatory mechanisms as stated above may also be involved in E-cadherin gene repression in CRT-overexpressing cells, suggesting that further investigation is required.

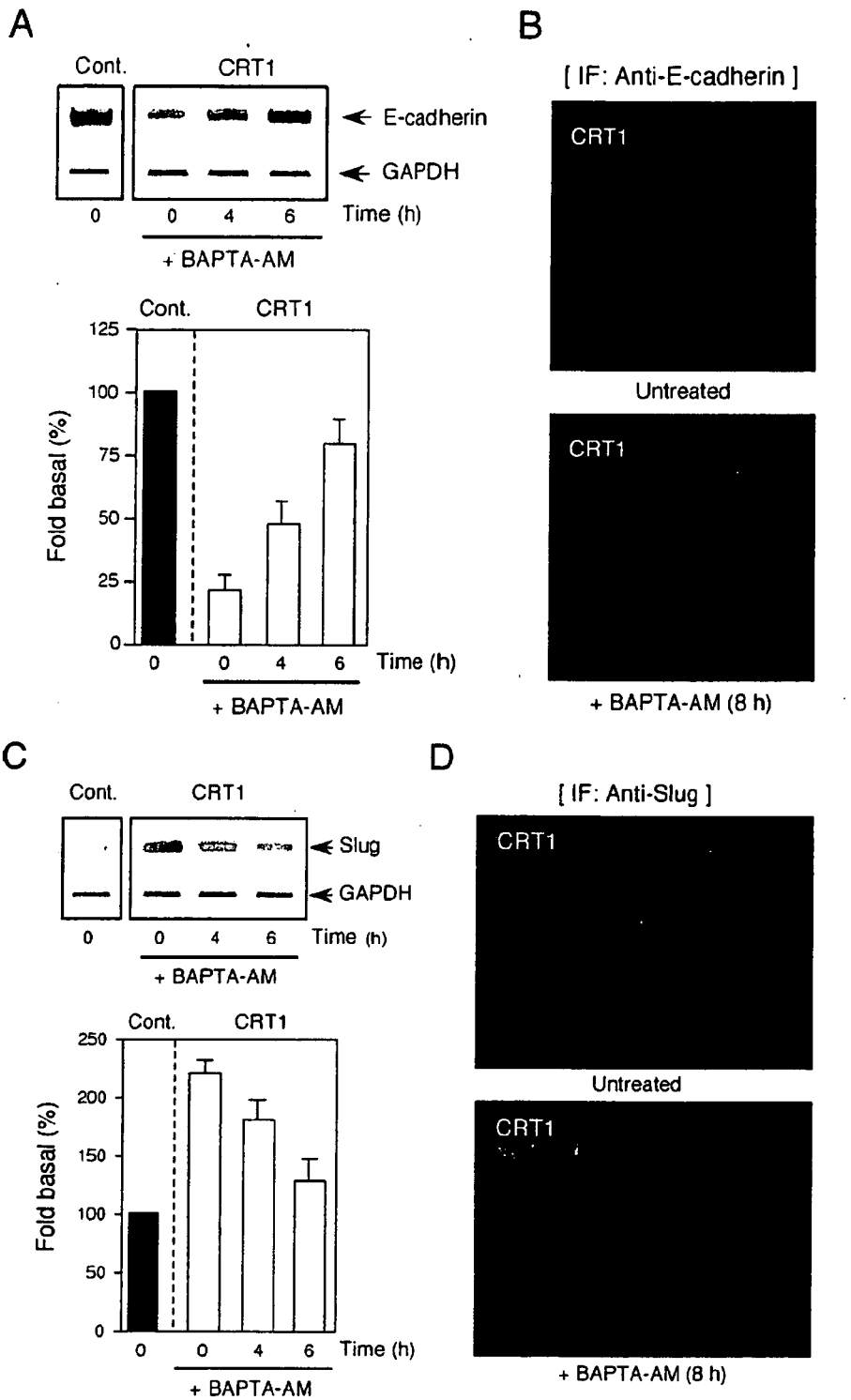

FIGURE 10. **BAPTA-AM, a Ca^{2+} chelator, up-regulated the expression of E-cadherin and down-regulated the expression of Slug in CRT-overexpressing cells.** *A*, MDCK-CRT1 cells were treated with BAPTA-AM (10 μM) for the periods indicated, and the level of E-cadherin expression was examined by RT-PCR analysis using specific primers. The RT-PCR for E-cadherin was also shown in untreated MDCK-Control cells. *B*, MDCK-CRT1 cells were treated for 8 h with BAPTA-AM as described in *A*, and the expression of E-cadherin was examined by immunofluorescence microscopy by using the anti-E-cadherin antibody. Data represent three independent experiments. *C*, MDCK-CRT1 cells were treated with BAPTA-AM as described in *A*, and the level of Slug expression was examined by RT-PCR analysis using specific primers. The RT-PCR for Slug was also conducted in untreated MDCK-Control cells. *D*, MDCK-CRT1 cells were treated for 8 h with BAPTA-AM as described in *A*, and the expression of Slug was examined by immunofluorescence microscopy using the anti-Slug antibody. Data represent three independent experiments.

CRT modulates cell adhesiveness via the expression of N-cadherin and vinculin and affects Wnt signaling pathways in L-fibroblasts (58, 59). In that study, the authors found that CRT overexpression increased cell adhesion with a concomitant increase of N-cadherin and vinculin in fibroblasts. On the other hand, we found that overexpression of CRT in MDCK cells caused a loss of cell-cell interaction and induced cell migration through the Matrigel® (Figs. 1*B*, 3*A*, and 3*B*). In terms of the effect of overexpressed CRT on cell-cell interaction, the reason for the discrepancy is not yet clear. However, it is noteworthy that primary fibroblasts show a mesenchymal phenotype with less expression of E-cadherin, compared with the levels in the epithelial cell-like MDCK cells (23). This suggests that the basal mechanisms for cell adhesion and motility differ between these cell types. Despite the discrepancy in cell morphology, the expression of N-cadherin and vinculin was induced by overexpression of CRT in both fibroblasts (59) and MDCK cells (this study), indicating that the present result does not necessarily contradict previous findings using CRT-overexpressing fibroblasts, in respect of the expression of N-cadherin and vinculin (58, 59). Very recently, Afshar *et al.* (60) reported that cellular migration and binding to collagen type V were apparently suppressed in embryonic fibroblasts from CRT knock-out mice, indicating that the cellular level of CRT is important for the regulation of cell motility. Cell surface expression of CRT has been reported in several cell types (3). In addition, Goicoechea *et al.* (61) reported that cell surface CRT functions as a receptor for thrombospondin to contribute to focal-adhesion disassembly of the cell. Although it is not clear how cell surface CRT contributes to thrombospondin-mediated signaling and regulation for cell migration, no significant expression of CRT was observed on the surface of CRT-overexpressing MDCK cells. Taken together, these findings suggest that

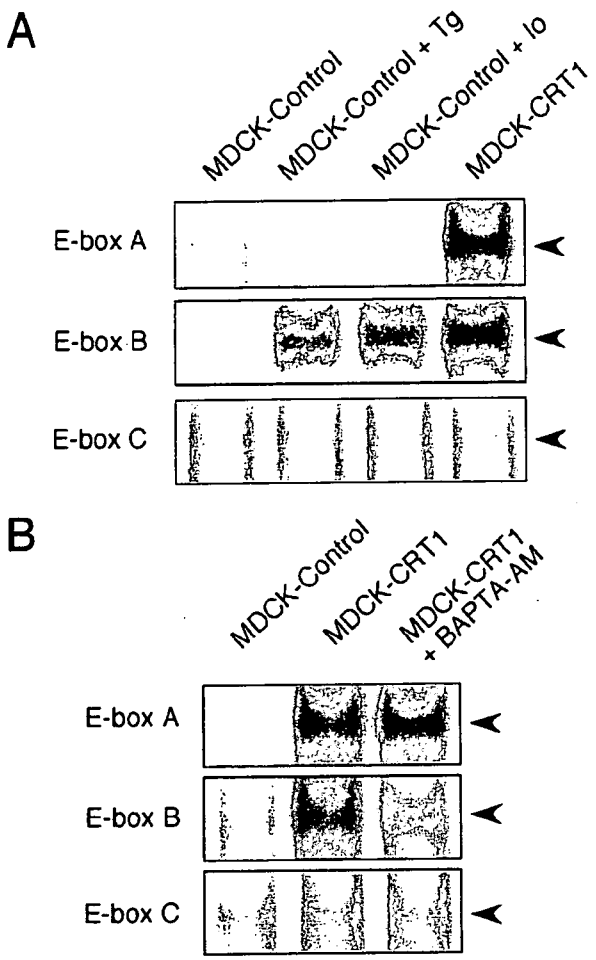

FIGURE 11. *A*, MDCK-Control cells were treated with or without thapsigargin (*Tg*, 5 μM) or ionomycin (*Io*, 1 μM) for 2 h, and nuclear extracts were prepared. The protein-binding activity of E-boxes was then examined by EMSA as described under "Experimental Procedures" using radiolabeled nucleotide probes for E-boxes A–C in the canine E-cadherin gene promoter. *Arrowheads* indicate shifted bands of protein complex with ^{32}P-labeled probes. Data represent three independent experiments. *B*, MDCK-CRT1 cells were treated with BAPTA-AM (10 μM) for 2 h, then nuclear extracts were prepared. The protein-binding activity of E-boxes was then examined by EMSA as described under "Experimental Procedures" using radiolabeled nucleotide probes for E-boxes A–C. Data represent three independent experiments.

CRT plays a vital role in the regulation of cell-cell interaction and cell motility in a variety of cell types.

E-cadherin appears to be an important target molecule in the mechanism influenced by CRT. To investigate the mechanism whereby CRT up-regulates the expression of Slug to repress the E-cadherin gene, we focused on Ca^{2+} homeostasis influenced by CRT overexpression in MDCK cells, because CRT plays an important role in the regulation of Ca^{2+} homeostasis in the ER (1). We found that thapsigargin-sensitive intracellular Ca^{2+} stores in the ER were apparently increased in CRT-overexpressing cells, compared with controls. This was consistent with previous reports concerning the intracellular Ca^{2+} stores in cells overexpressing CRT (13, 30, 62, 63). On the other hand, it has been reported that CRT modulates store-operated Ca^{2+} influx (1, 30, 64). In previous studies, decreased Ca^{2+} influx was observed in stable CRT-overexpressing cells (13, 30, 63), but not in cells transiently transfected with the CRT gene (65). In the present study, when the cells in Ca^{2+}-free medium were stimulated with thapsigargin, the level of $[Ca^{2+}]_i$ was apparently elevated more in CRT-overexpressing cells than controls. Then store-operated Ca^{2+} influx was examined by re-adding Ca^{2+} to the external medium, and the results showed that the $[Ca^{2+}]_i$ was significantly elevated in CRT-overexpressing cells compared with controls. This was unexpected and inconsistent with previous findings of the suppressive effect of CRT overexpression on store-operated Ca^{2+} influx (13, 30, 63). To explain why the Ca^{2+} influx was up-regulated by overexpressed CRT, the expression of several epithelial Ca^{2+} channels (*i.e.* TRPV5, TRPV6, and Polycystin 2) was examined in control and CRT-overexpressing cells. The results showed that, in CRT-overexpressing cells, the expression of TRPV5 was apparently up-regulated and the basal level of Ca^{2+} influx from external medium was also increased. TRPV5 and TRPV6 are highly Ca^{2+}-selective epithelial channels in the TRP cation channel superfamily, and they function to (re) absorb Ca^{2+} in the epithelial cells of specific organs, such as kidney, intestine, testis, esophagus, ileum, and colon (31). The causative relation between overexpressed TRPV5 and increased Ca^{2+} influx seen in CRT-overexpressing cells seemed to be consistent with previous findings in MDCK cells stably transfected with the TRPV5 gene (66). Recently, Pigozzi *et al.* (67) has reported that a change in Ca^{2+} stores in the ER influenced the gene regulation of some TRP channels, including TRPC1, TRPC3, and TRPV6 in a prostate cancer cell line, suggesting that the expression of these TRP channels may be regulated by alteration of cellular Ca^{2+} homeostasis. However, in the present study, it is not clear how the expression of TRPV5 is specifically up-regulated in the CRT-overexpressing MDCK cells. Taken together, these results suggest that stable overexpression of CRT in MDCK cells may cause an imbalance of Ca^{2+} homeostasis, and this leads to the up-regulation of TRPV5, resulting in the increase in the basal level of Ca^{2+} uptake. On the other hand, in previous reports, levels of $[Ca^{2+}]_i$ in the resting state were not significantly different between control and CRT-overexpressing cells (13, 30, 63). Thus, the up-regulation of the $[Ca^{2+}]_i$ state in CRT-overexpressing MDCK cells seems to be unusual compared with other cell types, and further investigation is required to clarify the mechanism involved.

To our knowledge, whether the expression of Slug is controlled in a Ca^{2+}-mediated manner has not been investigated. In this study, we showed that, in MDCK cells, the transcription of Slug was up-regulated by thapsigargin or ionomycin, which increased $[Ca^{2+}]_i$ (Fig. 9), leading to an increase in intensity of the gel-shift band of the protein-DNA complex of E-box B in the E-cadherin promoter (Fig. 11*A*). These results were consistent with the finding that E-cadherin expression was suppressed through the up-regulation of Slug expression in MDCK cells by treatment with thapsigargin or ionomycin. Conversely, in CRT-overexpressing cells treated with BAPTA-AM, the expression of Slug was suppressed and the expression of E-cadherin was increased. This indicates that the altered regulation of E-cadherin expression through Slug was dependent on an increased $[Ca^{2+}]_i$ in CRT-overexpressing cells. Collectively, these results strongly support the notion that overexpression of CRT suppresses E-cadherin expression by up-regulating Slug expression

through the increased level of Ca^{2+}. Zhao *et al.* (68) reported that the Slug gene is a downstream target of the transcription factor MyoD, and is up-regulated by MyoD through the E-boxes in its promoter. Furthermore, a Ca^{2+}-responsive E-box element, CaRE2, was identified to function in the transcription of the brain-derived neurotrophic factor gene in neurons (69), suggesting a possible regulation of the Ca^{2+}-induced up-regulation of E-box elements in the *Slug* gene. In terms of these findings, further investigation is required to clarify how the Slug gene is up-regulated by the increased $[Ca^{2+}]_i$ in CRT-overexpressing cells.

In terms of the relationship between CRT and cancer, proteomic analysis has revealed a new functional role of CRT for the early diagnosis of cancers. CRT is proposed as a new tumor marker of bladder cancer (70) and autoantibodies to CRT isoforms have utility for the early diagnosis of pancreatic cancer (71). These reactions are not indicative of malignant properties of CRT but, rather, are markers of immunogenicity and anticancer responses (72, 73). On the other hand, another report demonstrated that CRT is overexpressed in the nuclear matrix in hepatocellular carcinoma, compared with normal liver tissue, suggesting a relationship between overexpressed CRT and malignant transformation (74). In this study, we found that overexpression of CRT conferred migratory ability on epithelial-like MDCK cells. To gain invasive ability is a characteristic of malignancy, although the increase of invasiveness induced by CRT does not directly indicate that CRT is an oncogenic factor. MDCK cells transfected with an expression vector for the Snail gene, a zinc finger transcription factor like Slug, gained invasive and angiogenic properties through the repression of the E-cadherin gene and behaved like carcinomas (75). However, cell growth of Snail-overexpressing MDCK cells is less than that of control cells. These results are compatible with our present findings. In addition, a recent report indicated that Snail overexpression in MDCK cells up-regulated the matrix metalloproteinase-9 (*MMP-9*) gene, suggesting some contribution to cell invasiveness (76). Taken together, these findings suggest that CRT has a potential function to increase cell invasion by suppressing E-cadherin expression through zinc finger transcription factors like Slug, resulting in a contribution to the establishment of invasive characteristics in malignancies. To test this hypothesis, further investigations, including studies *in vivo*, will be required.

In conclusion, in the present study, we demonstrated a novel function of CRT in cell adhesion and motility of the epithelium. The enhanced cell invasiveness mediated through E-cadherin gene repression was regulated by the gene repressor, Slug, via altered Ca^{2+} homeostasis caused by overexpression of CRT in epithelial MDCK cells.

Acknowledgments—We are grateful to Midori Ikezaki and Akiko Emura for technical assistance.

REFERENCES

1. Michalak, M., Corbett, E. F., Masaeli, N., Nakamura, K., and Opas, M. (1999) *Biochem. J.* **344,** 281–292
2. Michalak, M., Robert, J. M., and Opas, M. (2002) *Cell Calcium* **32,** 269–278
3. Johnson, S., Michalak, M., Opas, M., and Eggleton, P. (2001) *Trends. Cell Biol.* **11,** 122–129
4. Gardai, S. J., McPhillips, K. A., Frasch, S. C., Janssen, W. J., Starefeldt, A., Murphy-Ullrich, J. E., Bratton, D. L., Oldenborg, P. A., Michalak, M., and Henson, P. M. (2005) *Cell* **123,** 321–334
5. Krause, K. H., and Michalak, M. (1997) *Cell* **88,** 439–443
6. Helenius, A., Trombetta, E. S., Hebert, D. N., and Simons, J. F. (1997) *Trends Cell Biol.* **7,** 193–200
7. Holaska, J. M., Black, B. E., Love, D. C., Hanover, J. A., Leszyk, J., and Paschal, B. M. (2001) *J. Cell Biol.* **152,** 127–140
8. Mesaeli, N., Nakamura, K., Zvaritch, E., Dickie, P., Dziak, E., Krause, K. H., Opas, M., MacLennan, D. H., and Michalak, M. (1999) *J. Cell Biol.* **144,** 857–868
9. Rauch, F., Prud'homme, J., Arabian, A., Dedhar, S., and St-Arnaud, R. (2000) *Exp. Cell Res.* **256,** 105–111
10. Imanaka-Yoshida K., Amitani, A., Ioshii, S. O., Koyabu, S., Yamakado, T., and Yoshida, T. (1996) *J. Mol. Cell. Cardiol.* **28,** 553–562
11. Nakamura, K., Robertson, M., Liu, G., Dickie, P., Nakamura, K., Guo, J. Q., Duff, H. J., Opas, M., Kavanagh, K., and Michalak, M. (2001) *J. Clin. Invest.* **107,** 1245–1253
12. Kageyama, K., Ihara, Y., Goto, S., Urata, Y., Toda, G., Yano, K., and Kondo, T. (2002) *J. Biol. Chem.* **277,** 19255–19264
13. Ihara, Y., Urata, Y., Goto, S., and Kondo, T. (2006) *Am. J. Physiol.* **290,** C208–C221
14. Waisman, D. M., Salimath, B. P., and Anderson, M. J. (1985) *J. Biol. Chem.* **260,** 1652–1660
15. Michalak, M., Milner, R. E., Burns, K., and Opas, M. (1992) *Biochem. J.* **285,** 681–692
16. Rodriguez-Boulan, E., and Nelson, W. J. (1989) *Science* **245,** 718–725
17. Hogeboom, G. H. (1955) *Methods Enzymol.* **1,** 16–19
18. Yoshimura, M., Nishikawa, A., Ihara, Y., Taniguchi, S., and Taniguchi, N. (1995) *Proc. Natl. Acad. Sci. U. S. A.* **92,** 8754–8758
19. Yasuoka, C., Ihara, Y., Ikeda, S., Miyahara, Y., Kondo, T., and Kohno, S. (2004) *J. Biol. Chem.* **279,** 51182–51192
20. Ohkubo, T., and Ozawa, M. (2004) *J. Cell Sci.* **117,** 1675–1685
21. Grynkiewcz, G., Poenie, M., and Tsien, R. Y. (1985) *J. Biol. Chem.* **260,** 3440–3450
22. Cano, A., Perez-Moreno, M. A., Rodoligo, I., Locascio, A., Blanco, M. J., Barrio, M. G., Portillo, F., and Nietro, M. A. (2000) *Nat. Cell Biol.* **2,** 76–83
23. Battle, E., Sancho, E., Franci, C., Dominguez, D., Monfar, M., Baulida, J., and Herreros, A. G. (2000) *Nat. Cell Biol.* **2,** 84–89
24. Thiery, J. P. (2002) *Nat. Rev. Cancer* **2,** 442–454
25. Kang, Y., and Massague, J. (2004) *Cell* **118,** 277–279
26. Nieto, M. A. (2002) *Nat. Rev. Mol. Cell. Biol.* **3,** 155–166
27. Peinado, H., Portillo, F., and Cano, A. (2004) *Int. J. Dev. Biol.* **48,** 365–375
28. Comijn, J., Berx, G., Vermassen, P., Verschueren, K., van Grunsven, L., Bruyneel, E., Mareel, M., Huylebroeck, D., and van Roy, F. (2001) *Mol. Cell.* **7,** 1267–1278
29. Hajra, K. M., Chen, D. Y., and Fearon, E. R. (2002) *Cancer Res.* **62,** 1613–1618
30. Arnaudeau, S., Frieden, M., Nakamura, K., Castelbou, C., Michalak, M., and Demaurex, N. (2002) *J. Biol. Chem.* **277,** 46696–46705
31. Hoenderop, J. G. J., Nilius, B., and Bindels, R. J. M. (2005) *Physiol. Rev.* **85,** 373–422
32. Luo, Y., Vassilev, P. M., Li, X., Kawanabe, Y., and Zhou, J. (2003) *Mol. Cell. Biol.* **23,** 2600–2607
33. Nijenhuis, T., Hoenderop, J. G. J., Van der Kemp, A. W. C. M., and Bindels, R. J. M. (2003) *J. Am. Soc. Nephrol.* **14,** 2731–2740
34. Takeichi, M. (1991) *Science* **251,** 1451–1455
35. Gumbiner, B. M. (1996) *Cell* **84,** 345–357
36. Gumbiner, B. M. (2005) *Nat. Rev. Mol. Cell. Biol.* **6,** 622–634
37. Wheelock, M. J., and Johnson, K. R. (2003) *Annu. Rev. Cell Dev. Biol.* **19,** 207–235
38. Vleminckx, K., Vakaet, L., Jr., Mareel, M., Fiers, W., and van Roy, F. (1991) *Cell* **66,** 107–119
39. Christofori, G., and Semb, H. (1999) *Trends. Biochem. Sci.* **24,** 73–76
40. Thiery, J. P. (2003) *Curr. Opin. Cell Biol.* **15,** 740–746
41. Huber, M. A., Kraut, N., and Beug, H. (2005) *Curr. Opin. Cell Biol.* **17,**

548–558
42. Christofori, G. (2003) *EMBO J.* **22,** 2318–2323
43. Hazan, R. B., Qiao, R., Keren, R., Badano, I., and Suyama, K. (2004) *Ann. N. Y. Acad. Sci.* **1014,** 155–163
44. Maeda, M., Johnson, K. R., and Wheelock, M. J. (2005) *J. Cell Sci.* **118,** 873–887
45. Hemavathy, K., Guru, S. C., Harris, J., Chen, J. D., and Ip, Y. T. (2000) *Mol. Cell. Biol.* **26,** 5087–5095
46. Bolos, V., Peinado, H., Perez-Moreno, M. A., Fraga, M. F., Esteller, M., and Cano, A. (2003) *J. Cell Sci.* **116,** 499–511
47. Sekido, R., Murai, K., Funahashi, J., Kamachi, Y., Fujisawa-Sehara, A., Nabeshima, Y., and Kondoh, H. (1994) *Mol. Cell Biol.* **14,** 5692–5700
48. Remacle, J. E., Kraft, H., Lerchner, W., Wuytens, G., Collart, C., Verschueren, K., Smith, J. C., and Huylebroeck, D. (1999) *EMBO J.* **18,** 5073–5084
49. Verschueren, K., Remacle, J. E., Collart, C., Kraft, H., Baker, B. S., Tylzanowski, P., Nelles, L., Wuytens, G., Su, M. T., Bodmer, R., Smith, J. C., and Huylebroeck, D. (1999) *J. Biol. Chem.* **274,** 20489–20498
50. Perez-Moreno, M. A., Locascio, A., Rodrido, I., Dhondt, G., Portillo, F., Nieto, M. A., and Cano, A. (2001) *J. Biol. Chem.* **276,** 27424–27431
51. Rosivatz, E., Becker, I., Specht, K., Fricke, E., Luber, B., Busch, R., and Hofler, H., Becker, K. F. (2002) *Am. J. Pathol.* **161,** 1881–1891
52. Yang, J., Mani, S. A., Donaher, J. L., Ramaswamy, S., Itzykson, R. A., Come, C., Savagner, P., Gitelman, I., Richardson, A., and Weinberg, R. A. (2004) *Cell* **117,** 927–939
53. Giroldi, L. A., Bringuier, P. P., de Weijert, M., Jansen, C., van Bokhoven, A., and Schalken, J. A. (1997) *Biochem. Biophys. Res. Commun.* **241,** 453–458
54. Littlewood, T. D., and Evan, G. I. (1995) *Protein Profile* **2,** 621–702
55. Berx, G., Becker, K. F., Hofler, H., and van Roy, F. (1998) *Hum. Mutat.* **12,** 226–237
56. Graff, J. R., Gabrielson, E., Fujii, H., Baylin, S. B., and Herman, J. G. (2000) *J. Biol. Chem.* **275,** 2727–2732
57. Lickert, H., Bauer, A., Kemler, R., and Stappert, J. (2000) *J. Biol. Chem.* **275,** 5090–5095
58. Opas, M., Pawlikowski, M. S., Jass, G. K., Mesaeli, N., and Michalak, M. (1996) *J. Cell Biol.* **135,** 1–11
59. Fadel, M. P., Szewczenko-Pawlikowski, M., Leclerc, P., Dziak, E., Symonds, J. M., Blaschuk, O., Michalak, M., and Opas, M. (2001) *J. Biol. Chem.* **276,** 27083–27089
60. Afshar, N., Black, B. E., and Paschal, B. M. (2005) *Mol. Cell. Biol.* **25,** 8844–8853
61. Goicoechea, S., Orr, A. W., Pallero, M. A., Eggleton, P., and Murphy-Ullrich, J. E. (2000) *J. Biol. Chem.* **275,** 36358–36368
62. Bastianutto, C., Clementi, E., Codazzi, F., Podini, P., De Giorgi, F., Rizzuto, R., Meldolesi, J., and Pozzan, T. (1995) *J. Cell Biol.* **130,** 847–855
63. Mery, L., Mesaeli, N., Michalak, M., Opas, M., Lew, D. P., and Krause, K.-H. (1996) *J. Biol. Chem.* **271,** 9332–9339
64. Xu, W., Longo, F. J., Wintermantel, M. R., Jiang, X., Clark, R. A., and DeLisle, S. (2000) *J. Biol. Chem.* **275,** 36676–36682
65. Fasolato, C., Pizzo, P., and Pozzan, T. (1998) *Mol. Biol. Cell* **9,** 1513–1522
66. den Dekker, E., Schoeber, J., Topala, C. N., Van der Graaf, S. F. J., Hoenderop, J. G. J., and Bindels, R. J. M. (2005) *Pfluger Arch.* **450,** 236–244
67. Pigozzi, D., Ducret, T., Tajeddine, N., Gala, J.-L., Tombal, B., and Gailly, P. (2006) *Cell Calcium* **39,** 401–415
68. Zhao, P., Iezzi, S., Carver, E., Dressman, D., Gridley, T., Sartorelli, V., and Hoffman, E. P. (2002) *J. Biol. Chem.* **277,** 30091–30101
69. Chen, W. G., West, A. E., Tao, X., Corfas, G., Szentirmay, M. N., Sawadogo, M., Vinson, C., and Greenberg, M. E. (2003) *J. Neurosci.* **23,** 2572–2581
70. Kageyama, S., Isono, T., Iwaki, H., Wakabayashi, Y., Okada, Y., Kontani, K., Yoshimura, K., Terai, A., Arai, Y., and Yoshiki, T. (2004) *Clin. Chem.* **50,** 857–866
71. Hong, S. H., Misek, D. E., Wang, H., Puravs, E., Giordano, T. J., Greenson, J. K., Brenner, D. E., Simeone, D. M., Logsdon, C. D., and Hanash, S. M. (2004) *Cancer Res.* **64,** 5504–5510
72. Basu, S., and Srivastava, P. K. (1999) *J. Exp. Med.* **189,** 797–802
73. Graner, M., Raymond, A., Romney, D., He, L., Whitesell, L., and Katsanis, E. (2000) *Clin. Cancer Res.* **6,** 909–915
74. Yoon, G. S., Lee, H., Jung, Y., Yu, E., Moon, H. B., Song, K., and Lee, I. (2000) *Cancer Res.* **60,** 1117–1120
75. Peinado, H., Marin, F., Cubillo, E., Stark, H. J., Fusenig, N., Nieto, M. A., and Cano, A. (2004) *J. Cell Sci.* **117,** 2827–2839
76. Jorda, M., Olmeda, D., Vinyals, A., Valero, E., Cubillo, E., Llorens, A., Cano, A., and Fabra, A. (2005) *J. Cell Sci.* **118,** 3371–3385

Calreticulin, a Molecular Chaperone in the Endoplasmic Reticulum, Modulates Radiosensitivity of Human Glioblastoma U251MG Cells

Tomohiro Okunaga,[1,2] Yoshishige Urata,[1] Shinji Goto,[1] Takayuki Matsuo,[2] Shingo Mizota,[1,2] Keisuke Tsutsumi,[2] Izumi Nagata,[2] Takahito Kondo,[1] and Yoshito Ihara[1,3]

[1]Department of Biochemistry and Molecular Biology in Disease, Atomic Bomb Disease Institute; [2]Department of Neurosurgery, Nagasaki University Graduate School of Biomedical Sciences, Nagasaki, Japan; and [3]Core Research for Evolutional Science and Technology, Japan Science and Technology Agency, Kawaguchi, Japan

Abstract

Radiotherapy is the primary and most important adjuvant therapy for malignant gliomas. Although the mechanism of radiation resistance in gliomas has been studied for decades, it is still not clear how the resistance is related with functions of molecular chaperones in the endoplasmic reticulum. Calreticulin (CRT) is a Ca^{2+}-binding molecular chaperone in the endoplasmic reticulum. Recently, it was reported that changes in intracellular Ca^{2+} homeostasis play a role in the modulation of apoptosis. In the present study, we found that the level of CRT was higher in neuroglioma H4 cells than in glioblastoma cells (U251MG and T98G), and was well correlated with the sensitivity to γ-irradiation. To examine the role of CRT in the radiosensitivity of malignant gliomas, the *CRT* gene was introduced into U251MG cells, which express low levels of CRT, and the effect of overexpression of CRT on the radiosensitivity was examined. The cells transfected with the *CRT* gene exhibited enhanced radiation-induced apoptosis compared with untransfected control cells. In CRT-overexpressing cells, cell survival signaling via Akt was markedly suppressed. Furthermore, the gene expression of protein phosphatase 2Acα (PP2Acα), which is responsible for the dephosphorylation and inactivation of Akt, was up-regulated in CRT-overexpressing cells, and the regulation was dependent on Ca^{2+}. Thus, overexpression of CRT modulates radiation-induced apoptosis by suppressing Akt signaling through the up-regulation of PP2Acα expression via altered Ca^{2+} homeostasis. These results show the novel mechanism by which CRT is involved in the regulation of radiosensitivity and radiation-induced apoptosis in malignant glioma cells. (Cancer Res 2006; 66(17): 8662-71)

Introduction

The management of patients with glioblastoma multiforme is difficult and poor results have led to a search for novel therapeutic approaches (1). Radiotherapy is the most effective adjuvant modality in the management of glioblastoma multiforme, doubling the median survival rate (2). Radiation-induced cell death is associated with a complex interaction of various factors. The cellular targets of radiation-induced apoptosis are the plasma membrane, cytosol, and nuclear DNA (3). The mechanisms of radiation-induced apoptosis have been studied extensively in terms of p53 status, the Bcl-2 gene family, the Fas-mediated pathway, the ceramide-mediated pathway, the caspase cascade, and the ataxia-telangiectasia-mutated gene (3–5). Nevertheless, it still remains unclear which macroscopic or molecular features determine the response of glioblastoma multiforme to irradiation. For instance, although most studies have shown an association between p53 status and the response to radiotherapy (6), no such association has been convincingly shown in glioblastoma multiforme patients (7).

Recently, it was reported that the Ca^{2+} of the endoplasmic reticulum and/or cytoplasm plays an important role in radiation-induced apoptosis in association with some of these mechanisms (8–12). In the p53 pathways, Ca^{2+} and S100B regulated p53-dependent cell growth arrest and apoptosis (8). Bcl-2 and related proteins interfere with intracellular stores and the release of Ca^{2+} (13). Moreover, ceramide induces an increase in the cytoplasmic Ca^{2+} concentration by releasing Ca^{2+} from intracellular stores and activating the capacitative Ca^{2+} entry pathway, and deletion of Ca^{2+} from stores is a key to the protective action of Bcl-2 against apoptosis (11). In ataxia-telangiectasia cells, the mobilization of Ca^{2+} either was absent or increased slowly postirradiation (14). These findings indicate that changes in intracellular Ca^{2+} homeostasis play a role in the modulation of apoptosis (15).

Calreticulin (CRT) was initially found as a Ca^{2+}-binding protein in the lumen of the endoplasmic reticulum (16). CRT is a multifunctional protein involved in many biological processes that include the regulation of Ca^{2+} homeostasis (16), intercellular or intracellular signaling, gene expression (17), glycoprotein folding (18), and nuclear transport (19). We found that overexpression of CRT enhanced apoptosis in myocardiac H9c2 cells under conditions inductive to differentiation with retinoic acid (20) or under oxidative stress (21). Moreover, CRT regulates p53 function to induce apoptosis by affecting the rate of degradation and nuclear localization of p53 (12). Furthermore, there have been few reports related to the molecular chaperones and radiation-induced apoptosis of glioma (22). However, it is still not clear whether CRT is involved in the regulatory mechanism for the radiation-induced apoptosis.

In the present study, we investigated the role of CRT in radiosensitivity and radiation-induced apoptosis, using human glioma cell lines. We show here that overexpression of CRT modulates the radiosensitivity of human glioblastoma cells by suppressing Akt/protein kinase B signaling for cell survival via alterations of cellular Ca^{2+} homeostasis.

Requests for reprints: Yoshito Ihara, Department of Biochemistry and Molecular Biology in Disease, Atomic Bomb Disease Institute, Nagasaki University Graduate School of Biomedical Sciences, 1-12-4 Sakamoto, 852-8523 Nagasaki, Japan. Phone: 81-95-849-7099; Fax: 81-95-849-7100; E-mail: y-ihara@net.nagasaki-u.ac.jp.
©2006 American Association for Cancer Research.
doi:10.1158/0008-5472.CAN-05-4256

Materials and Methods

Antibodies and reagents. Antibodies against CRT, calnexin, Grp94, and Erp57 were purchased from Stressgen Biotech Corp. (Victoria, British Columbia, Canada). The anti-Akt and antiphosphorylated Akt (Ser^{473}, Thr^{309}) antibodies were purchased from Cell Signaling Technology (Beverly, MA). The anti-protein phosphatase 2A catalytic subunit α (PP2Acα) antibody was from BD Transduction Laboratories (Lexington, KY). The antibodies against PP2A regulatory protein 65 (PP2A-RP65) and PP1a were from Santa Cruz Biotechnology (Santa Cruz, CA). The anti-glyceraldehyde 3-phosphate dehydrogenase (GAPDH) antibody was purchased from Chemicon International (Temecula, CA). The reagents used in the study were all of high grade from Sigma or Wako Pure Chemicals (Osaka, Japan).

Cell culture. Two human glioblastoma cell lines (U251MG and T98G) and a human neuroglioma cell line (H4) were used in this study. The U251MG cells were obtained from Human Science Research Resource Bank (Osaka, Japan). The T98G and H4 cells were obtained from American Type Culture Collection (Manassas, VA). These cells and the *CRT* gene–transfected U251MG cells were cultured in DMEM supplemented with 10% FCS in a humidified atmosphere of 95% air and 5% CO_2 at 37°C. The culture medium was replaced every 2 days.

Gene transfection and selection of cells. A full-length mouse CRT cDNA was cloned from total RNA of mouse RAW264.7 cells by reverse transcription-PCR, and cloned into the mammalian expression plasmid pcDNA3.1 (Invitrogen, Tokyo, Japan) as described before (20). Myr-Akt1 in pUSEamp(+), an expression vector for myristoylated Akt, was obtained from Upstate (Lake Placid, NY). The gene expression vectors were introduced into U251MG cells using LipofectAMINE Plus reagent (Invitrogen) according to the directions from the manufacturer. Stable transfectants were screened by culturing with 500 μg/mL G418. The cloned G418-resistant lines were then screened for expression of CRT. Two independent clonal cell lines (CRT-M5 and CRT-M6) found to express high levels of CRT upon immunoblot analysis were selected and used for the experiments.

Terminal deoxynucleotidyltransferase-mediated dUTP nick end labeling assay. Apoptosis was detected by flow cytometry with the terminal deoxynucleotidyltransferase-mediated dUTP nick end labeling (TUNEL) method (23) using an Apop Tag Plus fluorescein *in situ* apoptosis detection kit (Chemicon International).

Immunoblot analysis. Cultured cells were harvested and lysed in lysis buffer [20 mmol/L Tris-HCl (pH 7.5), 130 mmol/L NaCl, and 1% NP40 including protease inhibitors (20 μmol/L amidinophenyl methanesulfonyl fluoride, 50 μmol/L pepstatin, and 50 μmol/L leupeptin)]. Protein samples were subjected to SDS-PAGE and then transferred to a nitrocellulose membrane as described (21). The membrane was blocked and then incubated with the primary antibody in TBS containing 0.05% Tween 20. The blots were coupled with the peroxidase-conjugated secondary antibodies, washed, and then developed using the ECL chemiluminescence detection kit (GE Healthcare Bioscience, Tokyo, Japan) according to the instructions from the manufacturer.

Cell survival assay and analysis. The cells were trypsinized in a 0.05% trypsin/1 mmol/L EDTA solution and replated in specified numbers into 60-mm dishes for determination of colony-forming ability (24). One day after, these dishes were irradiated with a dose of 0 to 10 Gy. A ^{60}Co source was used for the γ-irradiation of cells. After 14 days of incubation, the contents of the dishes were stained with a Giemsa stain solution (Muto Pure Chemicals, Tokyo, Japan), colonies with >50 cells were counted, and the radiation-surviving fraction (plating efficiency of experimental group/plating efficiency of control group) was determined. Survival curves were generated by combining data from four independent experiments in accordance with linear-quadratic fitting (KaleidaGraph software 4.0).

Protein phosphatase assay. Protein Ser/Thr phosphatase activity was assayed photometrically using Ser/Thr Phosphatase Assay Kit 1 (Upstate), according to the directions from the manufacturer. The activity was assayed in the presence or absence of 10 nmol/L okadaic acid, and the okadaic acid–sensitive activity was estimated as PP2A-specific activity. The phosphopeptide (R-K-pT-I-R-R) was used as a phosphatase substrate. Protein concentrations were determined using a BCA assay kit (Pierce, Rockford, IL).

Northern blot analysis. The full-length rat PP1a catalytic subunit and PP2A catalytic α cDNAs were generously provided by Dr. Kunimi Kikuchi (Hokkaido University, Hokkaido, Japan; refs. 25, 26). A *Pst*I-*Sma*I fragment of 600 bp and *Eco*RI-*Pvu*II fragment of 680 bp were prepared from the cDNAs of PP1ac and PP2Acα, respectively, and used as cDNA probes. The probes were labeled with ^{32}P using a Random Primer Labeling kit (Takara Biomedicals, Shiga, Japan). The isolation of cytoplasmic RNA and Northern blotting were essentially done as described before (27).

Assays for release and uptake of Ca^{2+} in the cell. For the $^{45}Ca^{2+}$ release assay, cells were cultured for 48 hours with medium containing $^{45}Ca^{2+}$ (1 μCi/mL). After washing with Ca^{2+}-free Earle's balanced salt solution (EBSS; Invitrogen) containing 3 mmol/L EGTA, cells were detached from the culture plates with trypsinization buffer (0.25% trypsin and 0.02% EDTA in EBSS), and the cell suspensions were preincubated in Ca^{2+}-free EBSS at 37°C for 3 minutes and sequentially stimulated with thapsigargin (0.1 μmol/L), ionomycin (2 μmol/L), and monensin (2 μmol/L). The cell suspensions were collected 5 minutes after the addition of each reagent and centrifuged. The radioactivity released from the cells was measured in the supernatant. Cell pellets were lysed and protein amounts were determined using a BCA assay kit (Pierce). $^{45}Ca^{2+}$ release was expressed as the cpm subtracted from those recovered in the preceding collection, and normalized to the protein in the corresponding cell pellets. The uptake of Ca^{2+} was measured radiometrically using the Millipore filtration technique as described previously (21) with a slight modification. The cells were irradiated (5 Gy) for the periods indicated, then washed with EBSS and cultured for 10 minutes in EBSS containing $^{45}Ca^{2+}$ (5 μCi/mL). Cells were detached from the culture plates by trypsinization buffer, and the cell suspension was filtered through a 0.45-μm nitrocellulose filter (Bio-Rad, Tokyo, Japan) under vacuum conditions. The filters were rinsed twice with 0.5 mL washing buffer [10 mmol/L HEPES (pH 7.4), 150 mmol/L KCl, 2 mmol/L EGTA, and 2.5 mmol/L $MgCl_2$]. $^{45}Ca^{2+}$ uptake was calculated by measuring the radioactivity and standardized using protein concentrations.

Measurement of intracellular free calcium. The cytoplasmic free Ca^{2+} concentration, $[Ca^{2+}]_i$, was measured with a dual-excitation wavelength spectrofluorophotometer (RF-5500, Shimadzu, Kyoto, Japan) using the fluorescent Ca^{2+} indicator Fura-2 tetra (acetoxymethyl) ester (Fura-2-AM) essentially as described previously (21).

Luciferase activity assay. Luciferase reporter constructs for the rat PP2Acα gene promoter [i.e., pGL3-pro-PP2Ac, pGL3-pro-PP2Ac (C3), and pGL3-pro-PP2Ac (C3-Mut/C)] were prepared using the reporter vector pGL3-Basic (Stratagene, Tokyo, Japan) as described previously (27). Each vector was transfected into cells by using LipofectAMINE 2000 (Invitrogen) according to the instructions from the manufacturer. After 24 hours of transfection, cells were treated with thapsigargin (5 μmol/L) or BAPTA-AM (10 μmol/L) or left untreated for the periods indicated in the text. Then, luciferase activity was assayed with cellular extracts by using a Dual-Luciferase Reporter Assay System (Promega, Tokyo, Japan).

Statistical analysis. Statistical analysis was done using Student's *t* test or ANOVA (StatView software). Significance was set at $P < 0.05$.

Results

Radiosensitivity and expression levels of CRT in human glioma cell lines. To investigate whether the expression level of endoplasmic reticulum chaperones differs in accordance with the radiosensitivity of glia-derived malignant cells, human neuroglioma (H4) and glioblastoma (U251MG and T98G) cells were selected as different categories of glioma. First, to examine the radiosensitivity of each cell line, the colony-forming ability of the cells after γ-irradiation (0-10 Gy) was evaluated, as described in Materials and Methods. As shown in Fig. 1A, H4 exhibited a significant decrease in the surviving fraction after γ-irradiation, compared with U251MG and T98G cells. These results indicate that H4 cells are highly susceptible to irradiation compared with U251MG and T98G cells, suggesting that radiosensitivity differs in different categories of glioma. In Fig. 1B, the expression of endoplasmic reticulum